POWER STORAGE IN D OCEAN

D2.1. Design Report of the marinized SMES, detailing the geometry, general characteristics and calculation of the machine side converter.

Funded by the European Union

This project is funded by European Climate, Infrastructure and Environment Executive Agency (CINEA), under the powers delegated by the European Commission under grant agreement Project: 101096457 – POSEIDON - HORIZON-CL5-2022-D5-01.

Document Information	
Deliverable	Design Report of the marinized SMES, detailing the geometry, general characteristics and calculation of the machine side converter.
Lead Beneficiary	CYCLOMED
Type:	R -
Work Package	WP2 ESS 1: SMES Superconducting Magnetic Energy storage for marine applications.
Date	30/06/2023

Dissemination level

Dissemination Level	
PU: Public	
SEN: Sensitive, limited under the conditions of the Grant Agreement	X

History

Version	Date	Reason	Revised by
1	17/05/2023	First draft	
2	09/06/2023	Final Version	
3		Peer reviewed	
4		Final version submitted	

Author List

Organization	Name	Contact Information
CIEMAT	Luis García-Tabarés	Luis.garcia@ciemat.es
CIEMAT	Javier Munilla	javier.munilla@ciemat.es
CYCLOMED	Carlos Gil	c.gil@cyclomed.tech
CYCLOMED	Carlos Hernando	c.hernando@cyclomed.tech

Disclaimer

Funded by the European Union. Views and opinions expressed are however those of the author(s) only and do not necessarily reflect those of the European Union or EUROPEAN CLIMATE, INFRASTRUCTURE AND ENVIRONMENT EXECUTIVE AGENCY (CINEA). Neither the European Union nor the granting authority can be held responsible for them.

TABLE OF CONTENTS

EXECUTIVE SUMMARY

This Report constitutes the Deliverable 2.1 associated to Work Package 2 (Superconducting Magnetic Energy Storage for Marine Applications) which globally is devoted to the Technology Selection and the definition of the SMES characteristics and parameters, as stated in the POSEIDON proposal.

In order to define the required SMES for waterborne applications, the first activity to be performed was the analysis of potential SMES applications on board, considering that the electric power grids of modern ships have become more and more complex, including heavy loads as electric propulsion systems, heating, cooling, lightning, load manipulation and many others. At the end, the characteristics and dynamics of each load are unique, and the preservation of power quality has become challenging due to the distinct time constants, and ramping rates of the different components. The addition of an Energy Storage System (ESS) could provide benefits to the overall quality power system and particularly Fast Energy Storage Systems (FRESS) like SMES could be suitable to specific applications. In the report the potential of these systems is analyzed for different type of ships and its suitability considered. Secondly, the operational conditions in a maritime environment are analyzed in terms of applicable regulatory conditions and required specifications.

The next phase consisted in selecting each of the different subsystems constituting the SMES (Magnet, Cooling, Power Conditioning and Control and Protection) in a methodic approach according to functional, technological and operational conditions on board. Probably the most significant decision that has been taken is the use of a High Temperature Superconducting (HTS) Magnet with deep implications in the rest of subsystems.

Once decided to use a HTS magnet, the next task was to analyze the different alternatives for HTS materials, including suppliers and also alternatives for magnet global options and magnet specific configurations to conclude that the preferable choice is using a modular magnet based on double pancakes arranged in a solenoidal configuration with REBCCO tapes and using an intermediate permeability material core. Next, the calculation of the magnet was performed to determine geometrical, electromagnetic and mechanical parameters to fulfil the required specifications. This process globally provides the magnet geometry and also the magnet performances at different temperatures. A detection of the risky aspects of the magnet fabrication was performed and a concept design of experiments and a test rig to carry on them is presented in this deliverable.

Also, the thermal losses (including those derived from the pulsed operation of the SMES) are listed and calculated to allow finding a thermal budget to dimension the cooling system proposed for this application, which is based on a so-called Cryogenic Supply System, whose operation is also described.

Finally, the Power Conditioning System is selected from the three configurations that are possible: Thyristor-based, Voltage-Source and Current-Source, concluding that for this specific case a simplified version of the Voltage-Source is preferable.

1. SMES MARINIZATION

1.1. SMES APPLICATION ON BOARD

In 2016 most nations ratified, during COP21 Paris Climate Agreement, their commitment to achieve carbon-neutrality by the year 2050. The objective is ambitious and the only path to achieve it is through the electrification of the economy [1]. One of the key sectors is transportation, which is currently dominated by fossil fuels, and accounted, according to IEA, for 37% of CO2 emissions from end-use sectors in 2021 [2].

Maritime industry is no stranger to this phenomenon, and there is a well-stablished trend lead by the International Marine Organization (IMO), which has provided the industry with guidelines to reduce CO2, SOx and NOx emissions [3].

To achieve the environmental guidelines, electrifying the propulsion system and other service loads is the most frequently, and most effective, applied approach. Hence, modern shipboard microgrids have become complex systems due to the presence of high dynamic loads, complex control, and power management, similar to terrestrial islanded microgrids.

In order to accommodate all technology updates the grid architecture of ships has evolved: from a traditional radial power distribution architecture were propulsion and service loads were separated, to integrated power systems (IPS) where all loads share a common power system, to more recent architectures like zonal electrical distribution (ZED), including the possibility of using DC power systems for the advantages provided: enhanced control of power flow, use of alternative electrical machines for power generation which could provide weight savings, or the ease of integration of energy storage systems [4]. Figure 1 shows in a simplified schematic the difference in power electronics for a AC vs DC network for a cutter dredge.

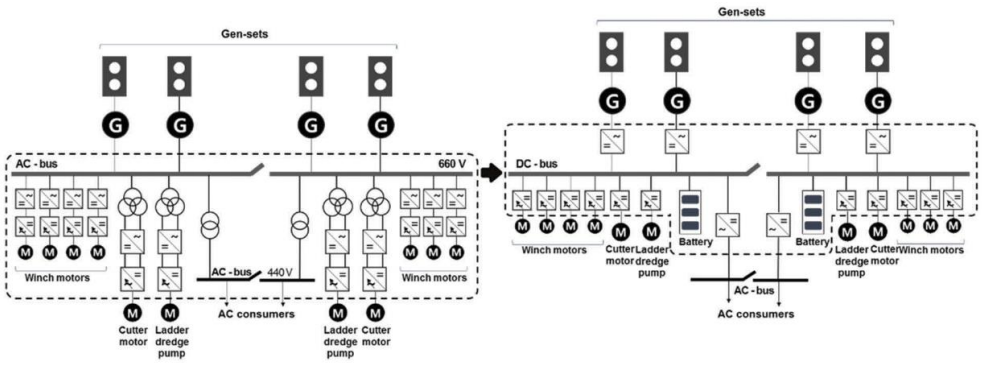

Figure 1. Comparison between the conventional AC network and a proposed DC network for a cutter dredge.

Modern architectures share, in the same power system, different types of loads:

- Propulsion Loads: Propulsion systems in vessels necessitate significant electrical power to operate. Electric propulsion systems, such as electric motors or thrusters, require substantial power inputs to propel the vessel through water. These loads typically constitute a major portion of the vessel's overall electrical consumption.
- Lighting Loads: Lighting plays a crucial role in vessel operations, ensuring adequate visibility for navigation, safety, and general functionality. Different types of lighting loads, such as general lighting, navigation lights, signal lights, and emergency lighting, are present throughout the vessel.
- Power and Auxiliary Loads: Numerous power-dependent systems are present in vessels to facilitate day-to-day operations. These auxiliary loads include electrical

equipment such as pumps, motors, compressors, fans, refrigeration systems, heating and ventilation systems, and communication equipment. They support various functions, such as fluid management, environmental control, and information exchange.

- Navigation and Communication Loads: Vessels rely on an array of navigation and communication systems to ensure safe and efficient operation. These systems may include radar, GPS (Global Positioning System), electronic chart displays, sonar systems, radio communication equipment, and other electronic aids. Such loads are essential for navigation, situational awareness, and effective communication with other vessels or shore stations.
- Control and Automation Loads: Modern vessels are equipped with sophisticated control and automation systems that enhance operational efficiency and safety. These systems, comprising programmable logic controllers (PLCs), distributed control systems (DCS), and other control devices, require electrical power to monitor, regulate, and automate various processes on board.
- Life Support Loads: Vessels accommodating crew and passengers need electrical loads to sustain life support systems. These loads encompass equipment such as air conditioning systems, water treatment systems, sewage treatment systems, and other facilities required for maintaining a comfortable and habitable environment on board.
- Emergency Loads: Emergency loads comprise essential systems that are activated during emergency situations. These loads may include emergency lighting, alarm systems, fire detection and suppression systems, emergency power supply equipment (such as emergency generators or battery backup systems), and other critical safety devices.

The characteristics and dynamics of each load are unique, and the preservation of power quality has become challenging due to the distinct time constants, and ramping rates, of the different components. The addition of an energy storage system (ESS) could provide benefits to the power system [5]:

- Improved power quality and stability: Energy storage systems can respond quickly to changes in the ship's power requirements, helping to regulate and stabilize the grid frequency and voltage. High variations of these factors can cause extreme equipment malfunction and safety issues.
- Lower operational costs: providing voltage and frequency support the ESS can help reducing fuel consumption allowing generators to operate at high efficient points.
- Load Leveling and Peak Shaving: Energy storage systems can help in load leveling by absorbing excess power during periods of low demand and releasing it during peak load periods. This optimizes the operation of onboard electrical systems and reduces the strain on power generation equipment, resulting in improved efficiency and fuel savings.
- Power Backup and Black Start Capability: Energy storage systems provide a reliable backup power source in case of a main power failure or emergency situations. They can ensure uninterrupted power supply to critical systems, such as navigation equipment, communication systems, emergency lighting, and life support systems. Energy storage systems with black start capability can also independently initiate power restoration after a complete blackout.
- Hybridization and Power Integration: Energy storage systems can be integrated with traditional power generation sources, such as diesel generators, to form hybrid power systems. By combining the intermittent power output of renewable energy sources (like solar or wind) with energy storage, these systems enhance overall power availability, reduce fuel consumption, and decrease emissions.

- Dynamic Positioning and Power Management: Energy storage systems are crucial for vessels equipped with dynamic positioning (DP) systems, which require rapid and accurate adjustments to maintain position. Energy storage enables quick power response, reducing the reliance on diesel generators, and enhancing fuel efficiency by operating them at optimal load conditions. It also provides power reserve for high-power-consuming operations, such as thruster maneuvering.
- Emission Reduction and Environmental Compliance: Energy storage systems facilitate the integration of renewable energy sources, such as solar panels or wind turbines, which help reduce the dependency on fossil fuel-based power generation. By minimizing the operation of combustion-based generators, energy storage systems contribute to lower greenhouse gas emissions, improved air quality, and compliance with environmental regulations.
- Ancillary Services and Grid Connection: Some vessels, such as offshore platforms or ships with significant power-generating capacity, can utilize energy storage systems to provide ancillary services to the electrical grid. These services may include frequency regulation, voltage support, peak shaving for onshore grids, or power supply during maintenance or repair work.

ESS technologies differ from each other in energy and power density, time response, charging/discharging rate. Presently there is no ESS that excels in every category, therefore there is work in the selection and optimization of the ESS in each application.

Currently high energy density ESS, such as batteries or fuel cells are being considered for different maritime projects [6]. However, their relatively low power density, slow response, and limited number of cycles does not make electrochemical batteries ideal for every application. Certain applications of ESS will require certain characteristics that are only achievable by a Fast Response Energy Storage System (FRESS) or a hybrid of certain ESS technologies. Figure 2 provides some an idea of ESS typical characteristics, at the top are the higher energy density systems and at the bottom the high-power density systems.

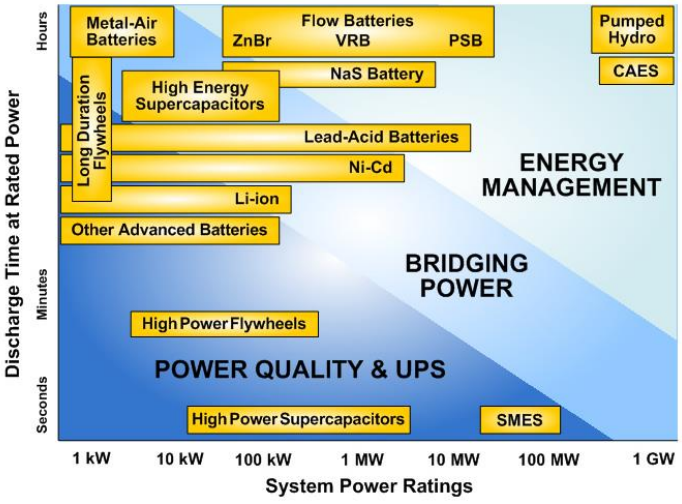

Figure 2. Energy storage technologies capacities [7]

FRESS energy systems, and specifically SMES, are characterized by:

- Very fast response;
- Unlimited number of number of charge/discharge cycles;
- Little or none degradation over time;
- Independency between power & energy;
- Operation at extremes temperatures;
- Uncritical deep discharge;
- No toxicity;
- Environmentally friendly

From these characteristics we have made an initial classification of the most attractive type of vessels for SMES integration based on data provided by the EMSA [8].

Table 1. Summary table of typical values for ESS technology requirements, and FRESS potential integration [8]

Ship type	C-rate	Cycles	Energy	FRESS potential
Ferry	Very high	Very high	Nominal	High
OSV	Very high	Very low	Nominal	Medium
Cruise	Low	Likely high	Very high	Medium
Offshore drilling unit	Very high	Variable	Low	High
Fishing vessel	Nominal	Nominal	Nominal	Medium
Fish farm vessel	Nominal	Nominal	Nominal	Medium
Shuttle tanker	Very high	Very low	Nominal	Medium
Short sea shipping	Highly variable	Highly variable	Highly variable	Medium
Deep sea vessels	Highly variable	Highly variable	Highly variable	Medium
Bulk vessels with cranes	High	High	Low	High
Tug boats	Highly variable	Highly variable	High min. space)	Medium
Yachts	Low	Low	High	Low
High speed ferry	High	High	High	High
Wind farm support vessels	Very high	Very low	Nominal	Medium

Validating this information [9] and [10] describe specific applications of Fast Response Energy Storage Systems in vessels. [9] shows the potential of introducing supercapacitors over Li-Ion batteries in a river ferry. And [10], shows how the inclusion of a FRESS could support the cranes of a bulk carrier vessel. From these use cases we can derive a range of energy and power values of interest for the SMES summarize in Table 2.

Table 2. Ranges of FRESS main parameters for maritime applications

	Min value	Max Value
Energy	100 kJ	100 MJ
Power	10kW	50 MW
Time constant (Energy/Power)	1 second	100 seconds

1.2. EXISTING MARINE REGULATORY CONDITIONS

Existing regulations for the implementation of energy storage in ships are primarily governed by international maritime organizations and classification societies. Here is a summary of the key regulations that have been detected for the WP2 development:

Organization	Description	Main references
International Maritime Organization (IMO)	The IMO, through its various conventions and codes, sets guidelines and standards for safety, environmental protection, and operational efficiency in the shipping industry. While energy storage systems are not explicitly addressed in specific regulations, they provide general guidelines to assure safety on-board.	[3]
Classification Societies	Classification societies, such as the American Bureau of Shipping (ABS), Lloyd's Register (LR), and DNV GL, provide rules and standards for the design, construction, and operation of ships. These societies have developed guidelines and certification procedures for energy storage systems on ships, ensuring their safety, reliability, and compliance with applicable regulations.	[11]–[13]
National and Regional Regulations	Different countries and regions may have their own regulations or guidelines for the implementation of energy storage in ships. These regulations can vary in terms of safety standards, operational requirements, and environmental considerations. Examples include the United States Coast Guard (USCG) regulations and guidelines issued by the European Maritime Safety Agency (EMSA).	[8], [14]
International Electrotechnical Commission (IEC) Standards	The IEC develops international standards for electrical and electronic technologies. Some relevant standards for energy storage systems on ships include IEC 62619 for secondary cells and batteries, IEC 62620 for secondary lithium-ion cells, and IEC 61851 for electric vehicle charging infrastructure.	[15]
Classification and Approval Process of R&D projects	Energy storage systems installed on ships typically undergo a classification and approval process by the relevant classification society. This process involves assessing the system's design, installation, safety features, performance, and compliance with applicable regulations. Once approved, the energy storage system receives classification and certification, which enables its installation and use on board.	[16]

It is important to note that the regulations and guidelines surrounding energy storage in ships are evolving as the industry explores new technologies and addresses emerging challenges, such as safety, fire prevention, and integration with existing ship systems.

1.2.1. FURTHER CONSIDERATION FOR A CORRECT MARINIZATION

Furthermore, as the marinization of SMES have not been previously approached, there are certain aspects from non-maritime organizations that need to be consider:

Organization	Description	Main references
Cryogenic Safety	SMES devices operate at cryogenic temperatures, typically utilizing liquid helium or liquid nitrogen for cooling. Compliance with cryogenic safety regulations and guidelines is crucial to ensure the safe handling and operation of the system. These regulations may cover aspects such as handling and storage of cryogenic fluids, ventilation requirements, and emergency response procedures.	[14]
Electromagnetic Interference (EMI) Regulations	SMES devices generate strong magnetic fields, which may interfere with nearby electronic devices and systems. Compliance with EMI regulations, such as those specified by the Federal Communications Commission (FCC) or equivalent local regulations, is necessary to minimize interference and ensure compatibility with other equipment.	[17]
Transportation Regulations	If the SMES device needs to be transported, consider transportation regulations for hazardous materials (if applicable) and follow proper procedures for packaging, labeling, and documentation. These regulations may include requirements for the transport of cryogenic fluids and other associated materials.	[14]

1.3. ESS SPECIFICATIONS

Based on recommendations from different sources [18] Table 3 summarizes the main specifications and parameters of the developed SMES for the POSEIDON project. Notice that all parameters are initial estimations for the design that will be presented in the next sections, and will be subject to future modifications.

Table 3. General information and technical specifications

Number	Subject	Description	Value (Estimates)
1	Enclosure Type	A description of the system enclosure, including any enclosure supplied with the system, provided as a part of the site installation and/or comprised of building assemblies associated with the installation	Stainless steel cryostat for the SMES. Electrical cabinets for the power electronics.
2	Equipment Footprint (m2)	L × W of system including all ancillary components	0.5x0.5 m2
3	Height (m)	Equipment height plus safe clearance distances above the equipment	2 m.
4	Weight (kg)	Weight of each individual subsystem (power conversion system ESS, accessories, etc.), including maximum shipping weight of largest item that will be transported to the project site	350 kg.
5	Operating Temperature Range (°C)	The ambient temperature range at which the system is designed to operate	-20-100°C

6	Grid Communication Protocols/Standards	List of communications-related protocols and standards with which the ESS is compliant	TBD
7	General Description of the Energy Storage System	Identification of the energy storage technology type (e.g., battery type, flywheel, etc.) used in the ESS	Superconducting Magnetic Energy Storage (SMES)
8	Warranty & Replacement Schedule	Warranty inclusions and exclusions, including replacement schedules and time span of warranty and any limitations	TBD
9	Expected Availability of System (%)	Percentage of time that the ESS is in full operation performing application-specific functions, taking into account both planned and unplanned down-time	> 90%
10	Rated Continuous Discharge Power (%/s)	The rate at which the ESS can continuously deliver energy for the entire specified SOC range of the storage device that comprises the ESS	10%
11	Rated Apparent Power (MW)	The real or reactive power (leading and lagging) that the ESS can provide into the AC grid continuously without exceeding the maximum operating temperature of the ESS	0.02 MW @ 4.2K
12	Rated Continuous Charge Power (MW)	The rate at which the ESS can capture energy for the entire SOC range of the storage device that comprises the ESS	0.02 MW @ 4.2K
13	Rated Continuous AC Current (discharge and charge) (A)	The AC current that the ESS can provide into the grid continuously and can accept from the grid continuously without exceeding the maximum operating temperature of the ESS	Not applicable for SMES. The rated DC current is: 0-520A
14	Output Voltage Range (V)	The range of AC grid voltage under which the ESS will operate in accordance with the ESS specification	700-1000 V
15	Rated Discharge Energy (Wh)	The accessible energy that can be provided by the ESS at its DC terminals when discharged at its beginning of life and end of life	70 Wh Lifecycle TBD.
16	Minimum Charge Time (s)	The minimum amount of time required for the ESS to be charged from minimum SOC to its rated maximum SOC	10 s

2. GLOBAL ALTERNATIVES FOR A MARITIME SMES CONFIGURATION

In general, a Superconducting Magnetic Energy Storage System (SMES) is a set of different Subsystems that constitute the whole device. In spite these Sub-Systems are globally common to every SMES, there are certain conditions for our particular SMES that limit or at least provide indications about what choices should be preferable.

Figure 3 shows the schematic configuration of a generic SMES in terms of the different Subsystems constituting it. These systems are:

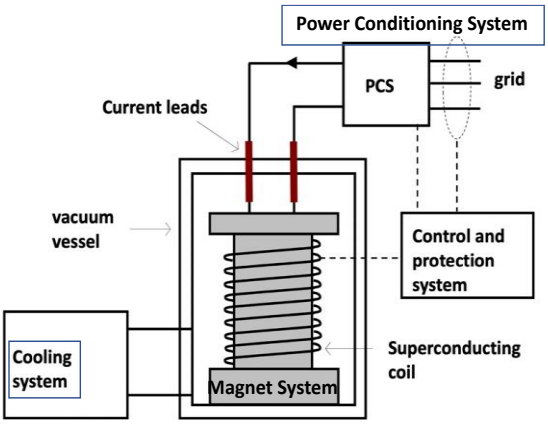

Figure 3. The different Subsystems of a SMES

1) The MAGNET Sub-System

2) The COOLING Sub-System

3) The POWER CONDITIONING Sub-System

4) The CONTROL & PROTECTION Sub-System

Figure 3 also includes some relevant components like the Superconducting Coil, the Currents Leads or the Vacuum Vessels, all of them included in the MAGNET System.

Besides the analysis of applications of SMES on-board that has been described in previous points, the core activity of this Work Package has been to define the selection criteria of each of the four Subsystems with special emphasis to the Magnet one.

To perform the analysis and the corresponding selection of options, some starting and global considerations are needed: Some are functional and include the required range of specifications, some others are technological and finally others are dictated by the operating conditions on-board. According to this statement, Table 4 shows the different variables associated to each of the group of selecting considerations.

Table 4. Variables to be considered for Selecting the SMES Sub-systems

SELECTING CRITERIA TYPE	VARIABLES TO BE CONSIDERED
Functional	Energy, Power, Voltage, Current, Operating Temperature
Technological	Superconductor type, Magnet configuration
Conditions On-board	Stray Field, Vibration Level and Inertia Loads, Environment, …..

The POSEIDON SMES selection is, obviously, affected by the three types of criteria shown in Table 4 but there is one consideration which becomes essential and, probably, the driving condition for choosing the different parts of the system. This consideration is the fact that the magnet will be based on High Temperature Superconductors (HTS) which implies that the magnet must be modular, made from the so-called double circular pancakes, which constitute the "bricks" for assembling the magnet. Unlike other magnets based on Low Temperature Superconductors LTS which can be wound in a continuous way and there is no need to make it modular, here the limitations of the HTS wires avoid using the same techniques and forcing the modularity of the magnet.

The choice of HTS is also essential for other Subsystems. Since the magnet will run at a higher temperature, there are more alternatives for cooling it, which are basically simpler and more economical but, on the contrary the use of HTS tapes makes difficult to reduce a.c. losses and this means that the amount of induced heat will be much higher with the subsequent impact on the cooling system.

There is another important implication of using an HTS magnet, affecting the Control and Protection System. Since quench propagation velocity is much smaller in HTS than in LTS, this will affect the detection system and also the protection one to avoid burning the magnet due to a high hot spot temperature.

Along the next subsections, the different options and decisions taken for each of the subsystems of the SMES are presented.

2.1. SMES MAGNET

2.1.1. SUPERCONDUCTING MATERIALS ALTERNATIVES

Superconductors, i.e., materials that exhibit superconductivity under specific conditions are numerous and are classified into type I or type II according to their behavior. Practically, almost only type II superconductors are used in engineering applications. Type II superconductors are further classified according to their critical temperature: low temperature superconductors (LTS) or high temperature superconductors (HTS). LTS have a critical temperature of less than 30 K. Their physics is well understood, and they are described by BCS (Bardeen Cooper Schrieffer) theory. The LTS of industrial use are niobium titanium (NbTi) and Niobium Tin (Nb_3Sn). MgB_2 is sometimes classified as LTS because its physical behavior is explained by the BCS theory, but sometimes it is classified as HTS because its critical temperature is 39 K. It is also defined as an intermediate critical temperature superconductor.

NbTi

Niobium titanium (NbTi) is the most common superconductor today. It represents 80 % of the superconductor market in the world (six billion dollars in 2017, about 3000 ton/a). It is a metallic alloy, easy to produce and quite inexpensive. For the production of NbTi wire, some NbTi billets are placed in a copper alloy or copper stabilizer and the whole is extruded, which is a classic process in metallurgy. In this way, it is easy to produce kilometer-long wires with micrometer strands in a stabilizer matrix (copper or copper alloy). Its T_C is 9.5 K and it is used in magnets that can provide a B-field up to 10 T at 4.2 K and 12 T at 1.8 K. It is therefore classified as LTS and is often used at 4.2 K (liquid helium at 1 bar) or 1.8 K (superfluid helium). NbTi is used, for example, in MRI and NMR magnets or for the dipoles of the Tevatron and the LHC. Moreover, NbTi has good mechanical properties which facilitates the fabrication of magnets with this material.

Nb_3Sn

Niobium-tin (Nb_3Sn) is also an LTS, but can be used to generate a higher B field. Its T_C is 18.3 K. Like NbTi, it has a simple crystallographic structure (A15 phase). There are two main processes for the manufacture of Nb_3Sn wire. In both cases in the beginning the conductor contains unreacted precursors (Nb and Sn), but not Nb_3Sn. The conductor is produced by the classical extrusion method, like NbTi. There are then two possibilities. The conductor is first heat treated to react the Nb_3Sn precursors to form Nb_3Sn filaments, which are then wound to form a magnet. If this is the case, the process is called react and wind. The other possibility, which is used more frequently, is to wind the magnet with the unreacted conductor, and then heat the coil to produce the Nb_3Sn filaments. The first process, "react and wind", is difficult because the reacted Nb_3Sn is a very brittle material and can break during winding. The "wind and react" process also has its

drawbacks because the performance of the superconducting material, and therefore the coil, is highly dependent on the quality of the heat treatment and its homogeneity, and the conductor shrinks during the reaction process. This shrinkage needs to be compensated in advance by applying a pre-stress to avoid loosening of the winding during heat treatment. In operation, Nb_3Sn coils expand more than NbTi coils. Nb_3Sn is used to make high field magnets (up to 23.5 T). It will be used for the central solenoid and toroidal coils of the ITER tokamak. Nb_3Sn-based magnets will also be used for the new LHC upgrade, "high-lumi", which aims to increase the luminosity of collisions.

MgB_2

MgB_2 (magnesium diboride) as a superconducting material has been a recent discovery, from 2001. It is more sensitive to magnetic field than Nb_3Sn but has a higher critical temperature, around 39 K. Today it is possible to buy kilometer-long MgB_2 conductors, which are quite inexpensive. They are produced by a process called PIT (Powder In Tube). In this process, some MgB_2 powder or its precursors (Mg and B) is filled into metal tubes, which are extruded and then assembled and re-extruded. The wire is then reacted to form the superconducting MgB_2 filaments. The performance improvement of MgB_2 in terms of current density is steadily progressing. Similar to Nb_3Sn, MgB_2 magnets can be wound by a react and wind or wind and react process. By the react and wind process, some limitations on the bending radius are appearing. Another drawback of MgB_2, is that due to the PIT process, the superconductor filaments are larger than NbTi or Nb_3Sn filaments, leading to higher AC losses.

BSSCO

BSCCO (Bismuth Strontium Calcium Calcium Copper Oxide), was in 1990 the first HTS to be implemented in a conductor. For that reason, BSCCO conductors are known as 1st Generation superconductors. Actually, there are 2 different compounds in the BSCCO Family that are used in commercially available conductors: BSSCO-2212 and BSSCO-2223. The TC of BSSCO-2212 is 85 K and the T_C of BSSCO-2223 is 110 K. BSCCO-2212 conductors are flat ribbon or round wires. BSSCO-2223 is only manufactured in the form of flat tapes. The tapes have anisotropic properties: IC depends on the orientation of the B-field with respect to the tape surface. BSCCO-2212 round wires have the advantage of isotropic properties and can be used to make cables with transposed wires (e.g. Rutherford cable), but with lower overall yields compared to tapes. BSSCO conductors are produced by the PIT process. The conductor matrix is silver, which has 2 disadvantages: - Silver is mechanically weak, requiring the conductor to be reinforced for applications under significant stress, such as high field magnets. - Silver is expensive, which limits the use of BSSCO tapes. Compared to REBCO conductors, BSSCO conductors have the advantage of being available in kilometer lengths, available as round cables and can be impregnated with epoxy resin. They are still under development, especially for very high field applications.

REBCO

REBCO (rare earth copper barium barium oxide) conductors or also referred to as second generation HTS conductors. They are part of the cuprate family, like BSSCOs. They are ceramics, arranged in a 2D structure. The rare earth used is either Yttrium or Gadolinium. Yttrium being the first to be used, the terms YBaCuO, YBCO or Y-123 are often used to refer to this family. REBCO conductors can exhibit high critical current densities even under high field, which makes them very interesting for the construction of high-field superconducting magnets. The T_C of YBaCuO is 93 K. REBCOs are fabricated as ribbons. The basic idea is to deposit the SC layer on a textured layer. There are two main options: The first uses a Nickel alloy substrate textured by mechanical and thermal treatments. However, a buffer layer is required to avoid reaction between the superconductor and

Ni. This option is known as RABiTSTM (Rolling Assisted Biaxially Textured Substrates). The second option (IBAD, ISD) uses a non-textured substrate, often Hastelloy on which a textured layer (YSZ, MgO) is deposited. Then, the superconducting layer is deposited directly or through intermediate layers. The REBCO layer, which is usually 1 or 2 µm thick, is created by a process called epitaxy. It is then plated with silver to protect the REBCO layer. The Ag layer facilitates oxidation. Additionally, a copper layer can be added either by lamination or electroplating for stabilization purposes. Currently, REBCO conductors are produced by about ten companies worldwide. Their manufacturing process may differ, but mainly some PVD (Physical Vapor Deposition) techniques are used. The price of REBCO tapes is relatively high and the conductor lengths are short, the conductor lengths sold are generally in the range of 100 m to 200 m.

Other drawbacks of REBCO tapes are the very low peeling strength of the superconducting layer, the lack of homogeneity of properties along the superconductor and the lack of reproducibility. Despite all these drawbacks, REBCO tapes are extremely interesting and their development is still in progress. Their price is currently decreasing, almost by a factor of two every two years and worldwide production is growing. Some new processes are being developed for REBCO layer growth, based on chemical methods. Although the properties of conductors obtained with these processes are not yet known to be as good as those obtained with PVD, rapid progress is observed. Above all, this deposition method has the potential to drastically reduce the manufacturing cost of REBCO conductors.

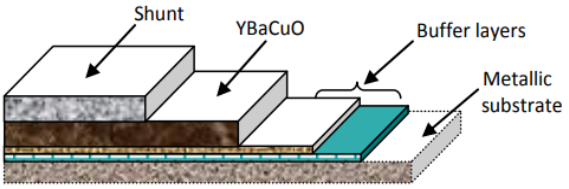

Figure 4. Structure of YBCO conductor [1]

Superconductor and provider selection

High-temperature superconductors (HTS) and low-temperature superconductors (LTS) have distinct characteristics that make each of them suitable for different applications:

- Higher critical temperatures: HTS materials can achieve superconductivity at relatively higher temperatures compared to LTS. While LTS typically operate at temperatures close to absolute zero, 4.2K (-273.15°C), HTS can exhibit superconductivity at significantly higher temperatures, typically below 77-100K. This higher critical temperature makes HTS more practical for certain applications that require less extreme cooling.
- Simplified cooling requirements: The higher critical temperature of HTS allows for the use of less costly and complex cooling systems. HTS materials can be cooled using liquid nitrogen, which is readily available and less expensive compared to the liquid helium used to cool LTS. This makes HTS more accessible and reduces the operational costs associated with superconducting devices.
- Enhanced magnetic field properties: HTS materials often exhibit stronger magnetic field capabilities than LTS. They can withstand and maintain superconductivity in higher magnetic fields.
- Improved current-carrying capacity: HTS materials have the potential to carry higher current densities than LTS.

For maritime applications the cooling requirements of LTS magnets are unachievable and for a viable long term development, and potential disruptor of the industry, we consider HTS as the better alternative in this case.

We have made a preselection of 3 potential suppliers of high temperature superconductors: Theva, Shanghai superconductors, and Sumitomo. The first two provide REBCO tape, and the partners of the project have experience with them as they have

collaborated in the past in other projects. Previous experience is key, as there is always certain R&D needed when you start working with a new supplier and we understand that this is out of scope for this project. The third one, Sumitomo, provides BSCCO tape and although the partners have not collaborated with them in the past it was included in order to have a full picture of the HTS landscape. Table 5 provides a comparison of the main mechanical properties of each HTS from the selected suppliers.

Table 5 Main mechanical properties of the superconducting tape provided by Theva, Shangai superconductors and Sumitomo.

PROPERTIES	Theva Pro-Line	Shanghai SC 2G REBCO	Sumitomo
Substrate	50 µm Hastelloy	30-50 µm Hastelloy	Type H - No reinforcement Type HT - Reinforced (SS, Copper, Nickel)
Buffer Layer	MgO	MgO + Others	-
Superconductor	GdBaCuO	REBCO 2G (GbBa2Cu3O7/EuBCO/YGdBCO)	BSSCO
Width	12 / 6 / **4** / 3 mm	10/ **4** / 3.3/ mm	4.5+-0.1 mm
Average thickness	0.11 + 0.05/0.1 mm Cu foil (laminated)	0.065-0.095 +- 10% mm Cu Plating	Type H - 0.23 +-0.01 mm.
		0.205-0.255 +-10% mm Cu lamination	Stainless Steel 0.29 +-0.02 mm.
	0.11 + 0.01/0.02 Cu surround (plated)	0.215 +-10% mm SS304 lamination	Copper Alloy 0.34 +- 0.02 mm.
			Nickel alloy 0.31 +- 0.03 mm
Minimum Bending Radius	20 mm	6-7 mm CU Plating	Type H - 80 mm.
			Stainless Steel 60 mm
		7-10 mm Cu Lamination	Copper Alloy 60 mm
		7-10 mm SS304 Lamination	Nickel alloy 40 mm
Maximum Handling Force	50 N for 12mm tape	-	Wire tension 80 N
			Wire tension 230 N
			Wire tension 280 N
			Wire tension 410 N
Maximum Rated Stress	165 to 500 MPa	100 MPa Cu Plating	Stainless steel - 20um : 270 MPa tensile strength 0.4% critical strain
		300-400 MPa Cu Lamination	Copper - 50 um: 250 MPa tensile strength 0.3% critical strain
		>700 MPa SS304 Lamination	Nickel alloy - 30um: 270 MPa tensile strength 0.4% critical strain
Piece Length (max)	25 to 200 m	< 1000 * m	Type H - < 1500 m.
			Type HT - < 500 m.
Insulation	Not provided	2 Kapton 25 µm width tapes overlapped	-
Price	32 €/m (depends on stock) + packaging & shipping for 100/200 m (short lengths for their production)	25-30 $/m \\ 23-28 €/m for S+ (medium grade) and a length 100 m. Double the length 40-50% more expensive.	20-30 $/m \\ 23-28 €/m

Among the mechanical properties of the superconductor 3 are essential from the design point of view: minimum bending radius which limits the coil dimensions, maximum rated stress which puts a mechanical limit on the tape stress, since the current dramatically decreases if surpassed, Figure 5, and the maximum available length of superconductor, which adds another constraint to the geometrical optimization of the coil.

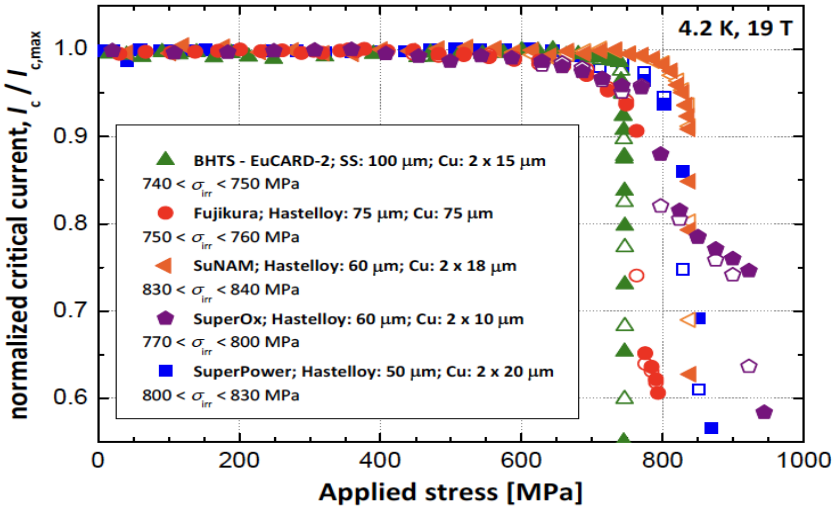

Figure 5. Normalized critical current Ic/Ic,max versus longitudinal tensile stress, σ, and irreversible stress limits, σirr, at 4.2 K and 19 T for five industrial REBCO tapes [19]

The electromagnetic properties of the tape of each supplier are different, Figure 6 and Figure 7 provide a comparison of such properties. Figure 6 shows the J-B-T for 3 selected temperatures (20-30-77K) and up to a magnetic field of 10T. In this case the tape provided by Shanghai superconductors shows better transport current capabilities, as it can transport approximately twice the current than Theva tape, and 10 times Sumitomo tape.

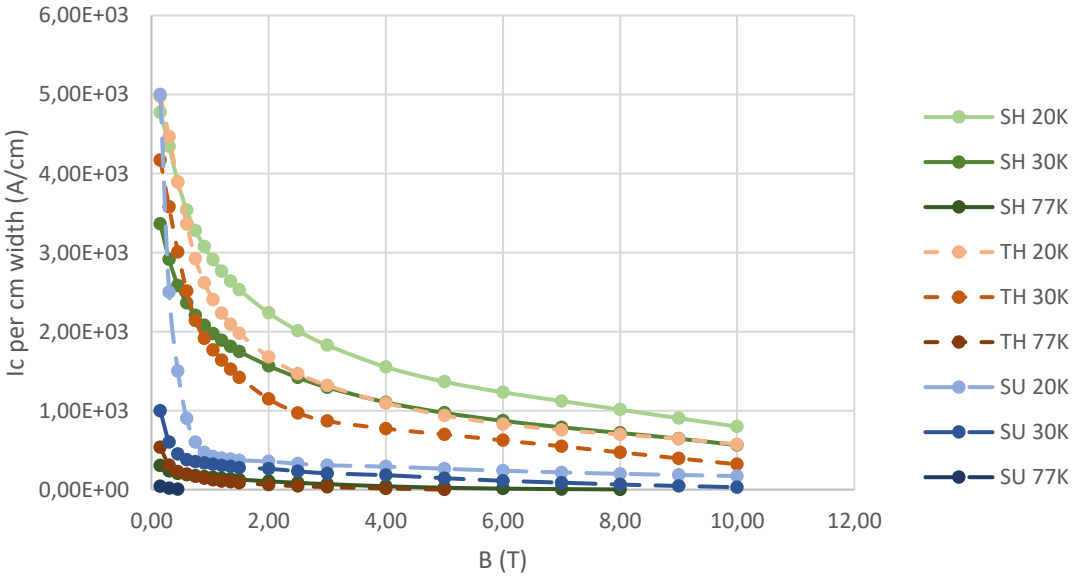

Figure 6. Current density as function of temperature and field for 3 HTS tapes

For the design of a SMES the product of B (Magnetic field) and J(Current density) provides a maximum for the specific energy of the SMES. Figure 7 shows this limit, from which we

can draw similar conclusions as before, as we can observe that Shanghai Superconductors tape provide better electromagnetic properties.

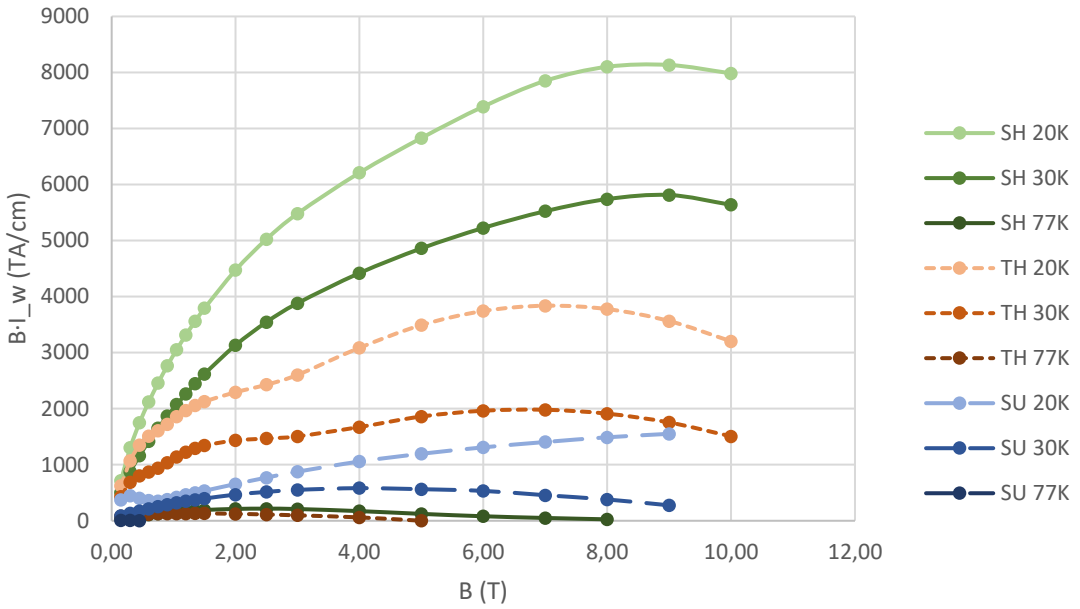

*Figure 7. B*I curve for the 3 selected superconducting materials*

Stating the main properties and characteristics of the selected superconducting tape we must decide on the provider that fulfills or better addresses the goals expected for the project. In Table 11we summarize and compare the most important design variables. Based on this comparison we decide that the best candidate as tape supplier is Shanghai superconductors.

Table 6 Main parameters for the computation of thermal losses

	Theva	Shangai Superconductor	Sumitomo
Mechanical			
Bendling radius	20 mm	✓ 6-7 mm: should be as small as possible as it will facilitate tape handling without degradation	70 mm
Handling force	50 N	-	✓ 230 N: Should be as large as possible as it allows to wind under tension to reduce EM forces
Rated stress	165-500MPa	✓ 300-700MPa: the larger the higher EM forces will withstand.	<300MPa
Available length	25 to 200 m	✓ < 1000 m: The larger the less joints	Type HT < 500 m.
Electromagnetic	Good	✓ Very Good	Bad
Economics	Bad	✓ Good	✓ Good

Experience	CYCLOMED and CIEMAT have certain experience in the operation of short lengths of tapes. But never manufactured a coil.	✓ ANTEC has experience in manufacturing coils. CYCLOMED and CIEMAT in the handling of short lengths	None: the fabrication of the coils should probably be subcontracted

2.1.2. ALTERNATIVES FOR THE SMES MAGNET

As already stated, the most important feature of a SMES magnet is its capability to produce a magnetic field in the convenient volume. Nevertheless, this is actually the way in which the energy is stored, and when the capabilities of adsorbing and releasing this energy at a given rated power are also considered, the most critical features of the system are defined.

Magnetic fields are related to currents according to electromagnetism, which result in the use of coils as the most convenient way for handling the magnetic fields. They give the possibility of using small and standard wires carrying small currents multiplied by the desired number of turns during the winding process, this is the main strength of a coil configuration for producing a magnetic field.

This scheme, quite well known and extensively used for so many applications using magnetic fields produced by resistive conductors is basically copied for the superconducting versions. The main differences arise from the point of view of the operational parameters: a superconducting coil can take profit of a higher current density. This results in higher magnetic field while using smaller coils and no resistive heat load (Joule heating). The drawbacks include the low temperature specification, the material cost and the complexity of the electrical connections.

From all the existing possibilities for designing a coil, there are just a few of them which are well suited for a superconducting SMES based on HTS tapes from these points:

- High magnetic field in a large volume for better energy density
- Magnetic field homogeneity: total energy is related to the energy density along the whole volume, while the limit is usually set by the peak value in the coil.
- Given the state of the art on manufacturing superconducting HTS tapes, important limitations come from the maximum length and minimum bending radius values achievable on a commercial grade tape.
- While the properties of copper cables are perfectly fitted for winding coils (isotropic behavior, ductility, thermal conductivity, yield strength,…), HTS tapes are quite different from this point of view.

Because of these reasons, designs based on any complex shape for the windings are completely discarded for this project.

Considering no specific size for the coil at this moment, two approaches can be foreseen for the SMES, solenoid and toroid, and both of them share some similarities:

- They can produce a quite homogeneous field (proportional to the ampere turns per unit length) inside a certain volume.
- They are based, theoretically, in an arrangement based on azimuthal currents around a revolution axis (a line of a solenoid and a circle for a toroid).

- They need, for a real-life design of a single coil, to add certain tilt in the cable for the accommodation of the next turn, which is usually done by an axial displacement of the cable along the azimuthal path. This is clear, from the Figure 8to provide continuity between turns in the coil but is important to note that the azimuthal component of the current is the important one from the point of view of the magnetic field produced inside and therefore the energy storage capability.

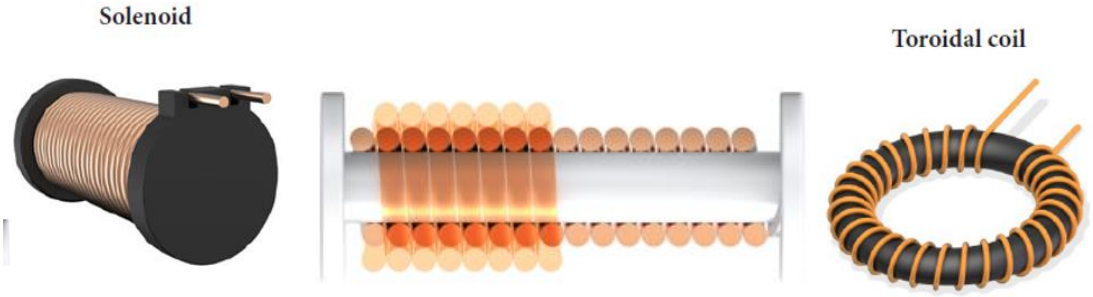

Figure 8. Basic arrangements for coil windings

If the HTS tape properties are taken into account, additional constraints are exposed and the magnet topology is further restricted:

- As stated in the previous chapter, the minimum bending radius of the tape is quite large. Moreover, this bending radius is dependent on the bending axis. There is no clear information from the suppliers about the minimum hard-axis radius and it can be considered much larger than the first one. This is an important point that results in discarding any coil designed using a reduced step value.
- A toroidal single coil is the worst from this point of view (a,b,c Figure 9), being the balanced toroidal coils slightly better but much more difficult to wind. A single solenoid with a large inner diameter compared to the tape width seems to be the best option from this point.

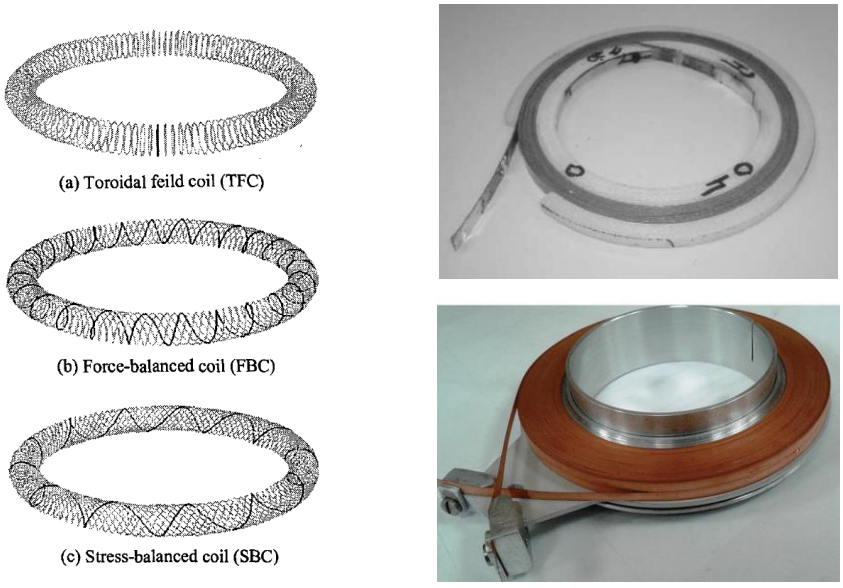

Figure 9. Coil design

A different approach for a coil design, is to wind the tapes without axial displacement (Figure 9, right side). This is the optimum situation from the point of view of the mechanical properties of the tape but would result in a very short coil. This is the pancake configuration and two options can be checked: Single or double pancake coil. The main

difference between both is the arrangement of the current leads. The single pancake has one current lead at the inner radius while the double pancake has both current leads at the outer radius, which is quite convenient for manufacturing.

Additional concept can be thought by using two single pancakes soldered at the inner surface. This is basically identical to the double pancake but it can produce a double size coil for a given length of tape. The drawback is the resistance of the soldered joint.

Once that the actual length of commercially available superconducting tape is defined, and based in the previous reasons, a concept based on a modular SMES is preferred. Moreover, a modular design based on pancakes fits almost perfect not only for a solenoid magnet but also for a toroidal magnet, while some additional advantages arise, like the scalability or robustness based on the easiness of a concept based on identical small components.

2.1.3. SMES MAGNET: HTS MODULAR SOLUTION

At present, the maximum available lengths in which HTS superconducting tapes are delivered hardily exceed 200m at the time there is a significant reduction of electrical properties as the length increases. Since the required length of tape for a useful application in a SMES can be in the order of several km, the only option is to fabricate the magnet from individual modules, electrically connected in series, which are called pancakes.

Figure 10 shows a schematic view of a double pancake which includes two single flat coils connected at the inner diameter (c) leaving the two external connections (A & B) at the outer diameter. There are basically two forms of connecting internally the two pancakes: One is soldering the two inner connections of each pancake and the other is making both pancakes (connected through a layer jump) at the same time with a special winding machine. Both of them will be described in more detail in a later section.

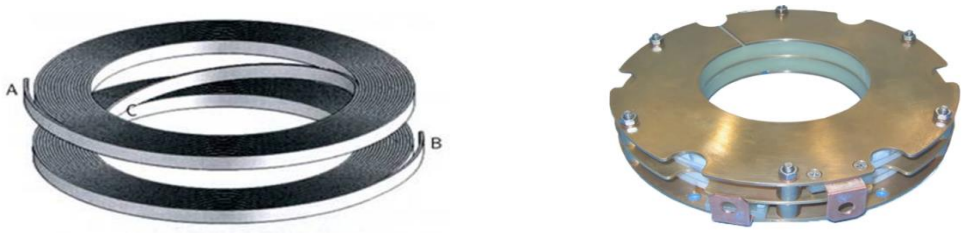

Figure 10 a) The concept of double pancake b) Double pancake manufactured by HTS110

Once the modular solution is chosen, options for the full magnet topology are very restricted, practically there are only two: The Solenoid and the Toroid, both with a circular or any other shape cross section.

Table 7 summarizes these two possible configurations in terms of pros and cons and also some alternatives to overcome or mitigate some of the drawbacks. In short, the toroid has a very small stray field and also the magnetic field component in the superconductor is mainly parallel to the tape broad side (which represents a better use of the tape), while it becomes a much more complicated magnet to manufacture, forces are not balanced in each pancake and the energy density, in terms of overall magnet volume, is significantly smaller than for the solenoid. On the contrary, solenoids have a much higher leakage field and the field component at the ends can be rather perpendicular to the tape broad side, reducing its critical current.

Table 7. Solenoid vs Toroid magnet options for SMES

	CONFIGURATION	ADVANTAGES	DISADVANTAGES	OPTIONS	
SOLENOID		* Simpler manufacturing * Apparently better energy density (Not clear for HTS) * Easier to manage Lorentz forces which are balanced	* High perpendicular B component at the coil ends > Lower J_c * High Stray Field, requiring active or passive shielding	* Arrangement of multiple solenoids to reduce the Stray Field	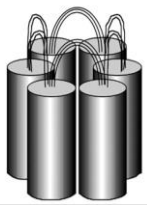
TOROID		* Very low stray field * Magnetic field rather parallel to the tape * Filling the bore with iron can increase the energy significantly.	* Not compensated net Lorentz forces in the coil. * More difficult cryostating * Apparently less energy density (J/kg)	* D-shape coils to cancel the coil unbalance	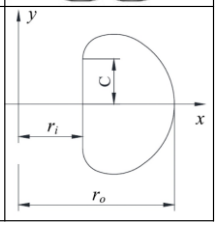

The situation can be improved for both options in different ways:

- The force unbalance in the coils of the toroid which lead to a net overall radial force in each coil, can be eliminated by making D-shape coils instead of circular ones (see Table 7). Nevertheless, the D-shape geometry is much more difficult to fabricate than the circular one, especially when HTS tapes are used.
- The high stray field in the solenoid can be reduced by arranging together several solenoids in a way that their respective return fields cancel each other. This solution also introduces an excessive complexity to the SMES System.
- Alternatively, the Solenoid can be equipped with an iron yoke that encloses most of the magnetic flux avoiding stray field away from the magnet. This solution has the additional advantage of reducing the unwanted component of the field perpendicular to the tape and increases its critical current.
- For both solutions, introducing a partial iron yoke, can increase the overall stored energy of the system.

Both configurations, the Toroid and the Solenoid with a high permeability iron core can be easily analyzed using some simplifications, basically the consideration of a one-dimensional magnetic field with a non-zero component only along the axis of the magnet (Figure 11).

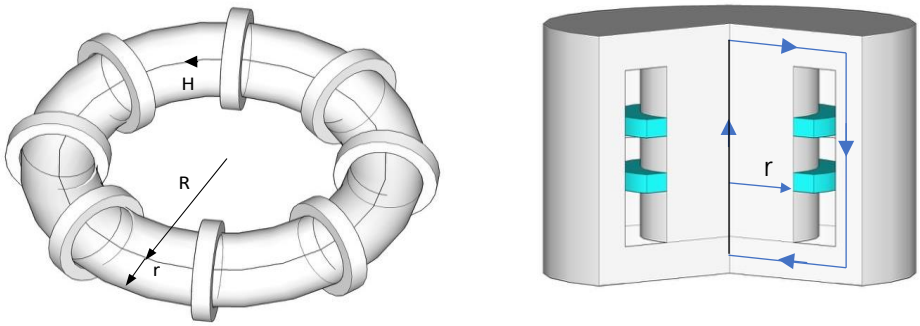

Figure 11 Toroidal geometry with circular section (left), solenoidal configuration with Iron Core Magnet with iron yoke (right)

Aplication of Ampere´s Law (see Figure 12) provides the value of the magnetic field strenght H, the peak flux density in the superconductor B_{SC} and the flux density in the core B_{CORE}:

$H=NI/L_h$ (electric load) (1.a)

$B_{sc} = B_{coreAIR} = \mu_0 \cdot NI/L_h$ (1.b)

$B_{coreIRON} = B(H)$ according to material´s properties (1.c)

The stored energy density will be generically expressed as:

$E_{core\ IRON} = \iiint \left(\int H(B) \cdot dB \right) \cdot dV$; According to the Iron H_B curve (2)

Which is graphically represented in Figure 12, also showing the co-energy of the system. As it can be observed, the energy density (Energy per unit volume of core magnet) is related to the area of the core H_B curve.

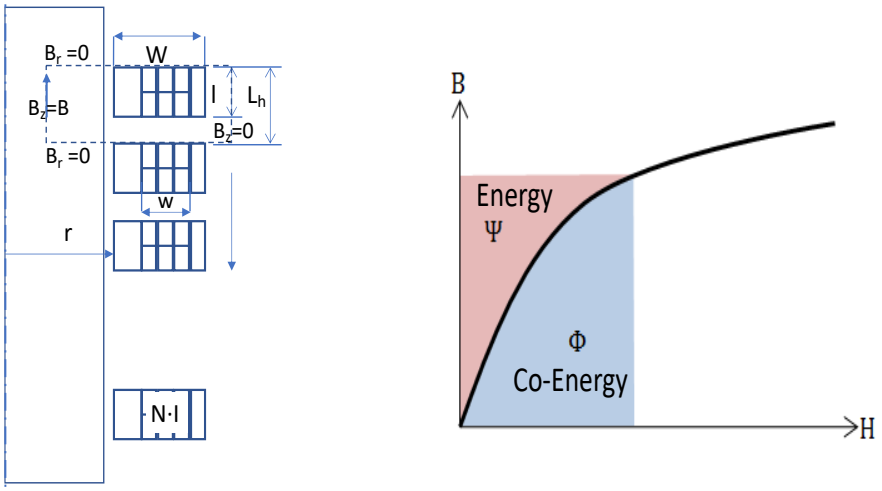

Figure 12 (Left) Modeling the Iron-Cored solenoid as an infinitely long solenoid (1D-Model, (Right) Graphical interpretation of the energy & co-energy density from the magnet core B-H curve

At this point our proposal is to make a cored magnet with a tailor-made H_B curve such that the stored energy is maximized or, in other terms, the magnet size minimized to achieve a certain energy. How are these intermediate permeability materials made? By interleaving layers of air and magnetic iron so that there is a volumetric proportion s of air to (1-s) of iron. Applying Ampere´s law to the complete magnetic circuits of length L shown in Figure 12, we get:

$H_e \cdot L = H_a \cdot s \cdot L + H_h(1-s) \cdot L$; $H_e(B) = H_a(B) \cdot s + H_h(B) \cdot (1-s) = (B/\mu_0) \cdot s + H_h(B) \cdot (1-s)$ (3)

Which establishes the procedure to calculate the equivalent $H_e(B)$ curve as a function of s. Figure 12 a, shows these curves for different values of s and also the areas corresponding to energy densities, for several values of the magnet electric load (H). For low values of H, small values of s provide higher stored energy levels while as the value of H increases, higher energy densities values are achieved at lower values of s. This is shown in figure 6b which represents the energy density as a function of H for different values of s. While for low values of H, the maximum energy density is achieved for full iron, as H increases, the maximum energy density is achieved for lower proportions of iron.

This concept is applicable either for solenoidal or toroidal magnets and is now under consideration and assessment for being patented.

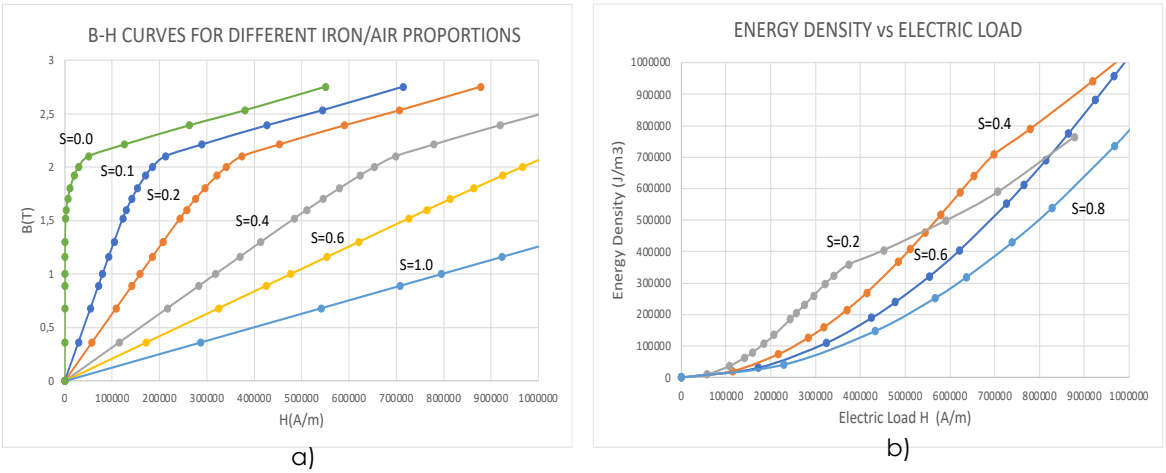

Figure 13. B-H curves (a) and Energy Density (b) for different Iron to Air proportions

From all the previous considerations explained along this section, and after a careful analysis of the different options, the solution that has been proposed is a solenoidal magnet with an adjustable permeability iron core to maximize the overall stored energy. The lower complexity of the magnet in terms of assembly, cooling and mechanical arrangement and its ability to become more compact has favored this decision. Nevertheless, we consider that the basis for both configurations is the same (the modular pancakes) and if in a later approach exploring the toroidal configuration is decided, great part of the work will be ready so far.

2.1.4. MAGNET CONCEPTUAL DESIGN

(1) ELECTROMAGNETIC DESIGN

Concept design

The concept design of the magnet starts after the evaluation of the different superconducting materials, every material has different properties, and the magnet has to be design according to these characteristics. The base concept of the magnet is a modular solenoidal magnet comprised of double pancakes as a basic module.

Base Case: Magnet comprise of N double pancakes

The base case of study will be a magnet with 12 double pancakes, each double pancake will be fabricated with 2 Shanghai Superconductors HTS tapes of 100 m length. The length of the tape is determined by the properties of the tape, a longer tape has higher risk of properties degradation. Once the length of the tape is determined, the geometric dimension of the double pancake must be established (outer radius, turns and inner radius).

The minimum inner radius for the pancake is limited by the tape properties, in the case of Shanghai superconductor tape, the minimum bending radius is 6-7 mm. According to these properties the minimum design radius for the pancake will be 10 mm, to avoid any degradation in the material properties.

The outer radius has some limits due to the fabrication process, bigger pancakes are harder to wind up and also requires bigger machines. With these precious factors, the base pancakes dimensions are:

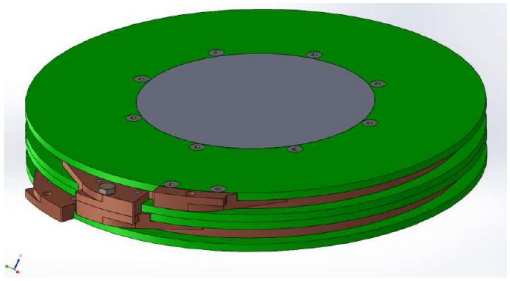

Parameters	Values
Outer radius	135 [mm]
Turns	144 [turns]
Inner radius	86 [mm]
Width	9.8 [mm]

Figure 14. Magnet comprise of N double pancakes

Electromagnetic optimization

The electromagnetic properties of the SMES are determined by the geometry of the magnet and the operation point, and both are related. Operation temperature, critical current and pancake distribution are some factors that affect the electromagnetic properties of the magnet. Different temperatures (4.2 K, 20 K, 65 K and 77.5 K) and space between pancakes (1 mm, 5 mm, 10 mm, 15 mm) will be studied. The process to optimize the magnet will be:

- Determinate the load curve of the magnet (J vs B curve) for each geometry configuration
- Compare the load curve with the critical current for each temperature to establish the operation point in each temperature.
- Analyze the operations points with FEM models.

The maximum magnetic field point in the magnet is usually used to determinate the load curve of the magnet, but as the HTS tapes has an anisotropic behavior, the angle between tapes and magnetic field is considered. The characteristic of the Shangai superconductor tapes makes it possible to differentiate only between 90º, (best performance) and the rest of the angles (worst performance).

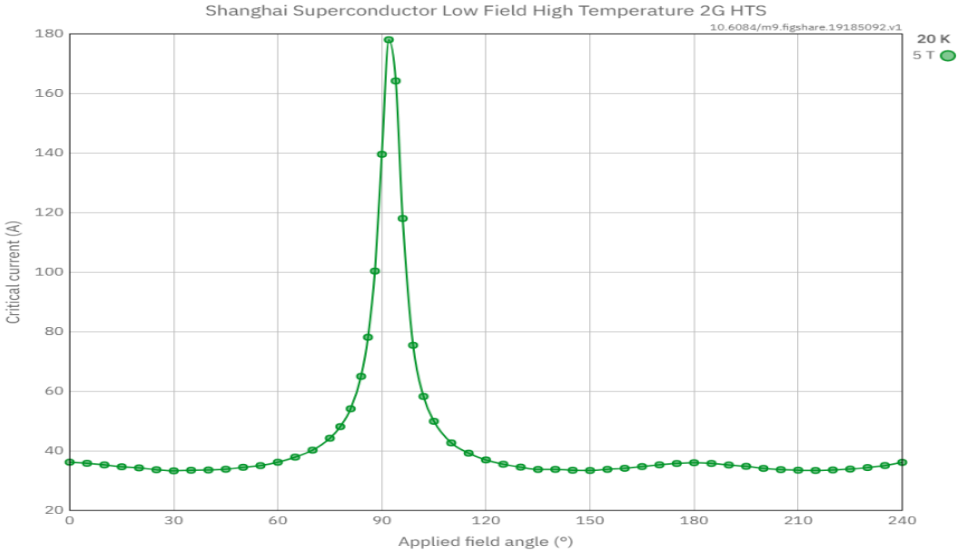

Figure 15. Shangai Superconductor HTS tape, critical current angle dependent

Angle dependence in the critical current of the HTS tapes makes it necessary to evaluate the load curve in the optimum point, 90º, and in the rest of the magnet. With the critical current vs angle curve, the magnet load including angle dependence can be established.

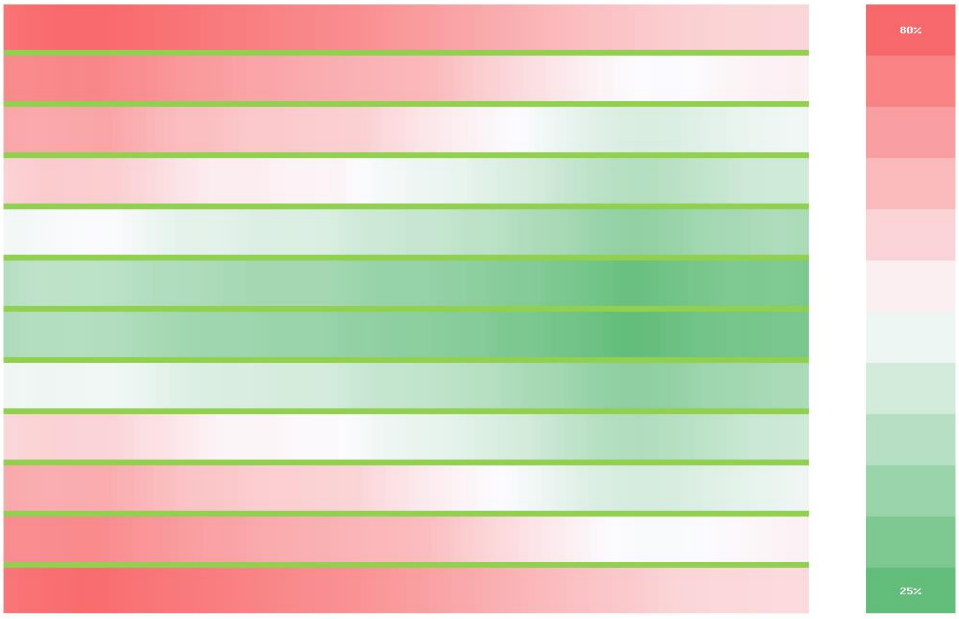

Figure 16. Magnet load

Figure 16 represents how close are each point of the magnet to the critical current, including the angle dependence between the magnetic field and the HTS tapes. Due to the anisotropy behavior of the tapes, the most critical point will be in the extreme of the magnet, first and last pancake, where the angle between magnetic field and tapes are lower, and the critical current for these points are lower.

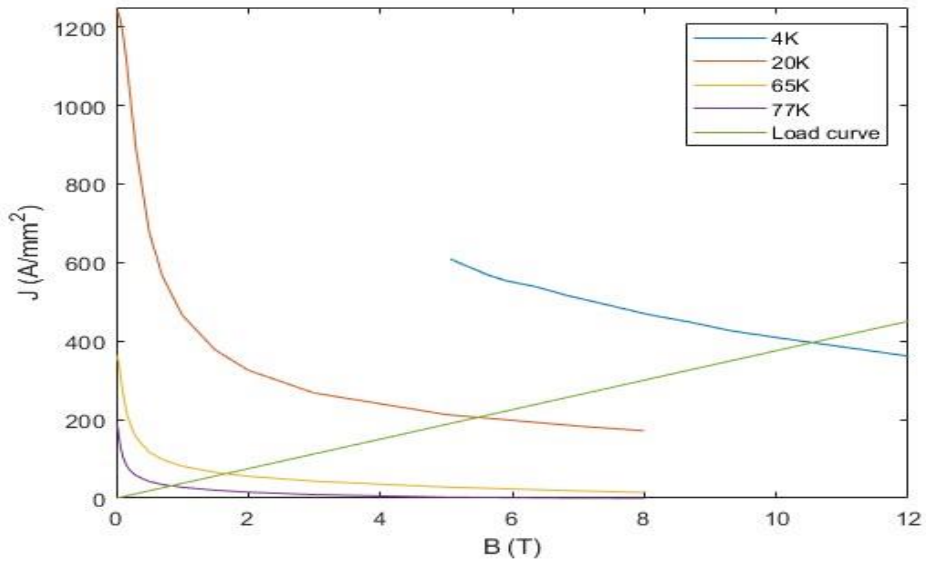

Figure 17: Critical currents and load curve for base configuration

Figure 17 represent the critical currents for different temperatures and the load curve for the configuration with 1 mm of separation between pancakes. The critical points are given by the intersection between the load curve and the critical curves of each temperature. The critical current is reduced to 80% to obtain the operating current. Table 8 shows the operating current density for each temperature and load case.

Table 8: Operating current density for different load cases

Pancake separation	Current density @ 4.2K [A/mm²]	Current density @ 20K [A/mm²]	Current density @ 65K [A/mm²]	Current density @ 77.5K [A/mm²]
1 mm	316.9	168.2	50.8	25.5
5 mm	342.0	178.8	54.4	27.5
10 mm	368.4	191.2	58.6	29.5
15 mm	389.3	200.3	61.7	31.3

Once the operating current is obtained, the energy storage of the system and the rest of the electromagnetic values are calculated by FEM analysis. Table 9 shows the total energy storage of the system at different temperatures, these values are obtained from the FEM analysis at the operating currents.

Table 9: Energy storage for different load cases

Pancake separation	Energy @ 4.2K [kJ]	Energy @ 20K [kJ]	Energy @ 65K [kJ]	Energy @ 77.5K [kJ]
1 mm	275.8	77.7	7.0	1.8
5 mm	272.4	74.4	6.9	1.7
10 mm	265.8	71.6	6.7	1.7
15 mm	256.4	67.9	6.4	1.6

As summary, the final electromagnetic concept design is a solenoidal magnet made up of **12 double pancakes** of 200 m length each one, able to operate up to 389 A/mm² and a maximum energy storage of **275.8 kJ at 4.2K**.

Protection

Quench protection [20] is something essential in the design of a superconducting magnet, in the case of HTS magnet, the protection is critical because the high specific heat and the characteristics of the HTS materials makes that the energy of the quench is dissipated in small points where the quench has occurred. The lack of propagation generates hot spots where the temperature in these points rises rapidly. When the temperature in the hot spots rises too much, the superconducting properties of the material are lost. To limit the temperature in the hot spots it is necessary an active protection of the magnet. The main method to protect an HTS magnet is to discharge the magnet when the quench is detected. This method dissipates the magnet energy in an external device and not trough the hot spot, it requires a fast discharge to reduce the risk of material degradation.

(2) MECHANICAL DESIGN

The mechanical stress distribution in a winding is not easy to evaluate, several approaches and suppositions can be made. In this study 2 different approaches are made, one analytical and other with FEM model.

Analytical stress

For a single thin turn with a current density J and submitted to a axial magnetic field B, the turn received a centrifugal force, this force results in a hoop stress given by:

$$\sigma = JBR$$

This formula is only valid for an individual turn without any contact with other turns or structure. The turns in a solenoid are not independent of each other, it is better to consider that the body of the solenoid suffers a volume density of the Laplace force and calculate the hoop stress and radial stress from this volume density force. The force to calculate the hoop and radial stress is obtained from the worst case of the electromagnetic design.

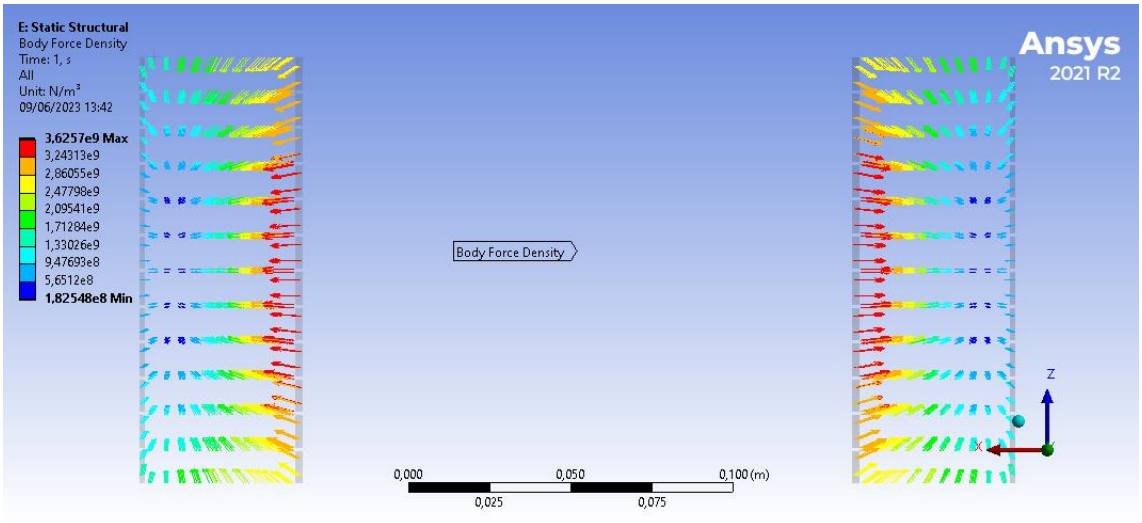

Figure 18: Body force density at 4.2K and 316 A/mm^2

Figure 18 shows the volume density force of the worst case scenario, at 4.2 K with 1 mm of separation between coils, in this load case the coil with higher forces and therefore higher stress will be the number 6, in the middle of the magnet.

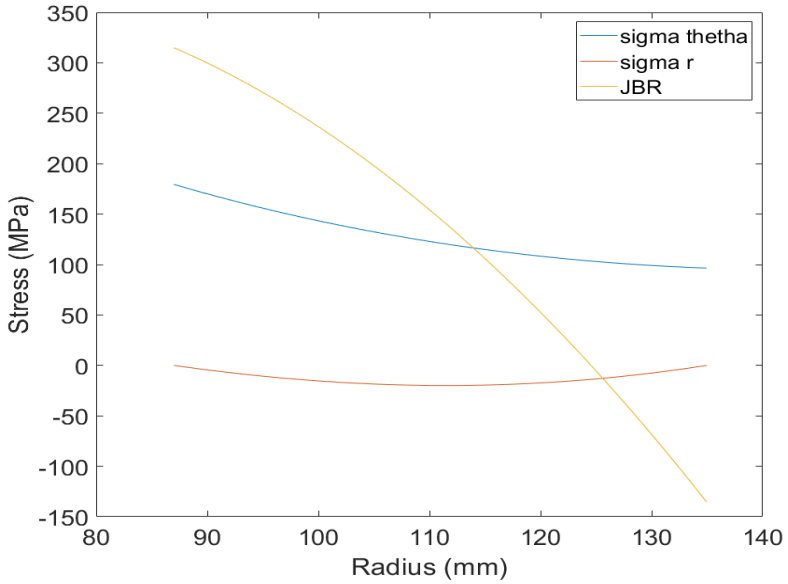

Figure 19: Stress vs magnet radius in coil N° 6

Figure 19 shows the stress in the middle coil of the magnet, in the worst case. The maximum hoop stress (sigma thetha) is lower than 200 MPa in the inner radius of the coil. Even if the JBR stress is evaluated, around 325 MPa, the stress in the coil is lower than the admissible stress of the tape, 400 MPa.

FEM analysis

FEM analysis evaluate the stress in the magnet using the volume density force of the Figure 18. The main difference between the analytical and the FEM analysis is that the FEM analysis needs to define the supports of the magnet.

At this stage of the project the final support structure is not developed, but the concept of the magnet and the support is to use some spacers between coils and fasten each other to maintain the position and orientation of the different coils. To reproduce this concept in the FEM analysis, 2 different boundary conditions are set. The first one is a 0-displacement condition in the upper and lower face of the coils, and the second boundary condition is to set contact between the coils, so all the coils behave as a single coil.

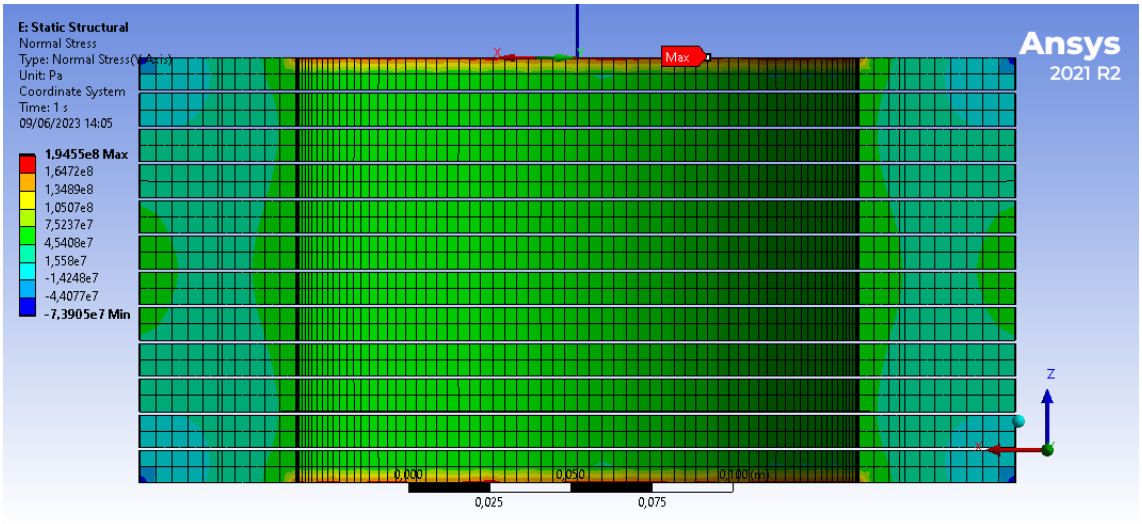

Figure 20: Hoop stress in Ansys at 4.2K and 316 A/mm^2

Figure 20 shows the result of the FEM analysis in the worst case, the hoop stress distribution is different than in the analytical analysis due to the boundary condition of 0-displacement. The maximum stress is 194 MPa, its found in the coils where the displacement are restricted and the value is similar than in the analytical analysis.

As summary, both analyses prove that the hoop stress in the magnet (< 200 MPa) are lower than the maximum admissible stress of the tape (400 MPa) for the worst case, where more energy is stored.

2.1.5. EXPERIMENTAL TEST BENCHES TO MEASURE RELEVANT DESIGN PARAMETERS

Several performance parameters of the HTS tape should be controlled, as there are a number of processes which could produce a degradation on their parameters. Some of them are handling, soldering, winding tension, thermomechanical stresses, but some other reasons could also be involved. All these points can be risky in terms of the tape performance for both the pair of soldered single pancakes and the double pancake (because of the layer jump).

Even more, the critical current of the tape should be checked in advance and the design of the current leads connectors could be also critical for the overall behavior of the coils. Therefore, a number of tests are foreseen, including a test bench for easy testing the main electrical features of the tape.

This test bench will be based on the minimum radius of the coil to be manufactured, and it will include the possibility to compare, under the same conditions, the layer jump for such a relatively small radius and the soldered joint between layers (Figure 21 left).

The soldering process will be also tested starting with the baseline of eutectic PbSn on the virgin tape. Different soldering materials based on Sn will be checked, with or without pressing the joint during the solder process and finally, the effect of sanding the tape for reducing the thickness of the joint (Figure 21, Right). This could be important not only for the soldered pancake approach, but also for the current leads design.

These tests will be done at liquid nitrogen temperature, which can be reached by means of a quite easy procedure and, at the same time, it will provide repeatability for the test series and a uniform constant temperature for the whole tape.

Some other parameters like the insulation of the tape along turns, thermomechanical effects on the mandrel material or winding tension, even when they are important for the coil design, will be not included in these tests as they are considered as second-order effect on the final decision between soldered single pancakes or double pancakes.

The measurements for every combination will include the voltage drop as a function of the current, the resistance of the joint and the current leads connections.

The mandrel and the tooling for handling the tapes are being manufactured in additive manufacturing (3D printer) for versatility. Nevertheless, additional tests could be needed for different radius of the coil to prove the correlation between the coil size and the electrical behavior of the tape.

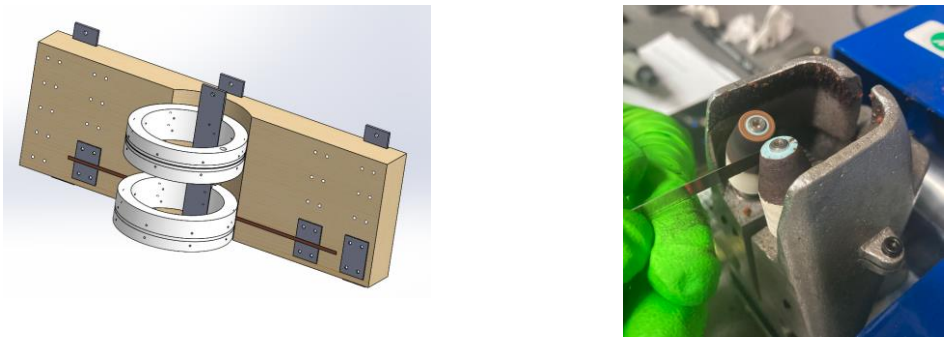

Figure 21. (Left) CAD design of the test bench of pancakes made of HTS tapes. (Right) Sanding process for the HTS tape for soldering testing

2.2. SMES COOLING SYSTEM

In this section we will develop the conceptual design of the cryogenic system of the superconducting coils assessing the temperature of operation, the sources of thermal losses, and the alternative configurations for the cryogenic system.

2.2.1. OPERATING TEMPERATURE

The operating temperature of a superconducting material is an important factor in the sizing of the cooling system to be used in the SMES. The efficiency of a cooling system cannot be higher than the Carnot efficiency, which is expressed by the following equation:

$$\frac{Q_c}{W} = \frac{T_c}{T_h - T_c}$$

Where T_h is the temperature of the hot focus and T_c is the temperature of the cold focus, W is the minimum work done by the system and Q_c is the heat extracted at low temperature from the system. Generally, the efficiency of refrigeration systems is well below the efficiency of a Carnot cycle. Figure 22 shows the exergy efficiency of each cooling technique as a function of temperature. The penalization of operating at lower temperatures is appreciated in this figure. It is not only more costly to operate at a lower

temperature due to a lower ideal COP, but also the proportion of the real COP to the ideal is also lower.

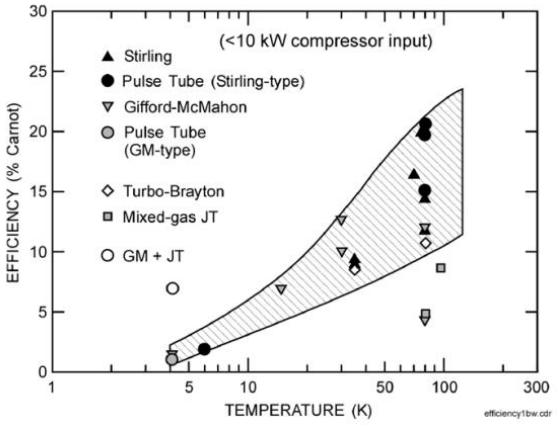

Figure 22. Efficiency as % of Carnot as a function of Temperature for selected cooling methods [21]

Initially we will consider 3 temperatures: 4.2K, 20K, and 77K, in line with the alternatives assessed in the electromagnetic design section.

2.2.2. THERMAL LOSSES

Having selected the temperature of operation we need to define the power of cryogenic system, for that reason the thermal losses of the system must be computed.

(1) THERMAL LOSSES: CONVECTION

Convection problems have a very clear solution that allows to reduce these losses in a very efficient way. They are reduced by simply maintaining a certain distance in vacuum between the material to be cooled and the cryostat wall, although they are not completely reduced, conduction caused by waste gases must be taken into account.

Once the vacuum pump has already reduced the pressure inside the cryostat and cooling has started, any residual gas inside the cryostat will condense on the cold surfaces, this condensation will depend on the species of gas present and the temperature of the surfaces. If, for example, the material is cooled by liquid Helium, at a temperature around 4.5 K, all the molecules that have not condensed will be Helium.

The composition of the residual gas will be practically pure helium. The residual gas regime according to the kinetic theory of gases [21] leads to the following transfer function that exists between two surfaces (T_1 cold temperature and T_2 hot temperature):

$$\dot{Q} = S_1 \alpha \theta \mathrm{p}(\mathrm{T}_2 - \mathrm{T}_1)$$

S_1 being the cold surface, α a coefficient that will depend on the types of gases, temperature and geometry, θ a coefficient dependent on the types of gases and p the pressure. This equation for the conduction of waste gases does not include the distance between the surfaces. This could be considered through the parameter a, but for ideal cases of large flat surfaces or concentric walls of similar radii, the thermal losses do not depend on the distance.

This leads us to try to optimize by reducing as much as possible the distance between the different layers inside the cryostat, as long as there is no contact between them, in order to allow a more compact solution.

Material choices

Outer shell: Stainless steel is preferred for the outer shell for several reasons including weldability, thermal contraction, corrosion resistance and emissivity at low temperatures. Additionally, it is important that the material for the cryostat is as much insensitive to the magnetic field as possible. For this later specification, austenitic stainless steel is the best choice. In terms of fracture toughness, some austenitic steels tend to become brittle at cryogenic temperatures. The best common austenitic steels for low temperatures while preserving ductile behavior are the series 304 and 316.

Fabrication guidelines

The SMES needs high vacuum for optimal thermal insulation. Therefore, clean surfaces are needed for all the parts in vacuum. Dust or grease on the surfaces is a potential problem for the vacuum system and the minimum achievable vacuum level. When possible, closed volumes should be avoided, as the trapped air will require a lot of time to be evacuated. E.g.: for joining two parts, it is preferred a bolt and a nut rather than a bolt screwed to a threaded blind hole.

Welding preparations will be designed in such a way that small volumes or clearances are not in the vacuum side of the assembly. The manufacturing procedures should include leak and pressure tests at intermediate steps of the fabrication and assembly to be sure that the welds are compliant with the vacuum specification.

(2) THERMAL LOSSES: CONDUCTION

The second mode of heat transfer is conduction through the supports of the cold mass. Thanks to Fourier's law, it is defined how heat is transmitted through solids, being proportional to the thermal conductivity constant of the material (k), to the cross section of the solid (A) and to a temperature gradient (∇T):

$$\dot{Q} = kA\nabla T$$

At cryogenic temperatures the thermal conductivity of the material becomes highly nonlinear and values for typical material structures span a wide range of several orders of magnitude. The most common approaches in the design of supports and vessels for cold material inside the cryostat include some heat transfer assumptions and make use of integral thermal conductivity [22].

According to Fourier's law, in order to try to reduce the thermal losses up to a certain value Q, the ratio between the length and the cross-sectional area of the support should be optimized (usually the area is reduced, and the length is increased).

This procedure can be enhanced by adding a thermal intercept. Typically, thermal intercepts are designed in one of the following ways:

1. A good thermal conductor is anchored to the intermediate temperature cooling system and then fixed in the right place at a certain position on the bracket.
2. The bracket is divided into two parts, inserted into an intermediate part, which is a good thermal conductor, and possibly attached directly to the intermediate cooler.

The second provides the best solution as it is able to trap all the heat coming from the hot side before it reaches the cold side of the support. The temperature homogeneity of this intermediate part is the key compared to the first mode, where the internal section of the support may not be sufficiently cooled.

Computation of conduction losses

The support will be the main source of conduction losses. For the design of the supports, the weight of the superconducting coils and the containment vessel must be considered.

Assuming that the load could have any direction, we proposed the following for the design of the supports:

1. A total of 4 G-10 CR supports are proposed. Which means that each rod will support ¼ of the total weight.
2. With a maximum stress for the G-10 composite of 400 MPa, the surface area of each rod should be at least the weight divided by the maximum stress multiplied by some safety coefficient.

The integrated thermal conductivity multiplied by the temperature difference, for 5K at 300K, is 153W/m. Whereas if these rods are anchored at 77 K (the integrated thermal conductivity multiplied by the temperature difference is 18 W/m).

Additional heat load would appear at 77 K (the integrated thermal conductivity multiplied by the temperature difference is 62 W/m).

(3) THERMAL LOSSES: RADIATION

The mode of heat transfer by radiation between two gray surfaces forming a closed enclosure is governed by:

$$q_{12} = \frac{\sigma(T_1^4 - T_2^4)}{\frac{1-\varepsilon_1}{\varepsilon_1 A_1} + \frac{1}{F_{12} A_1} + \frac{1-\varepsilon_2}{\varepsilon_2 A_2}}$$

Where σ is the Stefan-Boltzmann constant, T is the temperature, A is the surface area, ε is the emissivity, A is the area, and F is the viewing factor. The suffixes 1, 2, and 12 refer to surface 1, surface 2, and surface 1 to surface 2, respectively.

The heat transfer is proportional to the difference of the elevated temperatures to four. Therefore, it is more than desirable to establish one or more intermediate layers between the cryostat wall at room temperature and the outer wall of the cold mass of the cryostat. This is very common in cryostat design and is called heat shields. These could be actively cooled parts to dissipate heat more efficiently or simply parts that act passively in thermal equilibrium by radiative heat transfer:

- If passive heat shields are used, which are quite inexpensive and an easy way to reduce radiation losses, more than one layer is usually included. This is what is known as the multilayer insulation (MLI) concept, for which a reduction in thermal losses of the order of 1/(N-1) can be achieved where there are N layers [22] compared to the situation of having no shield at all.
- If an actively cooled heat shield is used, the values of thermal losses and steady state temperature can be custom designed. The physical parameters (emissivity, vision factor) and the cooling capacity turn out to be of importance for the performance of the heat shield. An additional advantage of using an active shield is the possibility of attaching a thermal interception to the shield support, so that the cooling used for the shield will also be used to reduce the conduction losses of the support.
- It is very common to combine both types of radiation heat shields. One layer of the refrigerated heat shield is covered by multilayer insulation. This is usually the best solution in terms of radiation insulation efficiency, while the most commonly used option, if there are no space constraints or thermal power limitations, simply makes use of passive multi-layer insulation.

Ideally, the material of an actively cooled heat shield should meet two conditions: good thermal conductivity and low emissivity. At the same time, its design should provide a homogeneous surface temperature to reduce temperature gradients at the coldest surface. The simplest design that meets the specifications is to have a path for the cryogen to cool the entire heat shield, for example, by bath cooling. If there is not enough space for such a bath, channels or pipes can be used to cool the shield as homogeneously as possible.

Computation of radiation losses

Simplifying the equation used above, the radiation losses could be calculated as:

$$Q = \sigma \varepsilon A (T_1^4 - T_2^4)$$

With the addition of a heat shield cooled to 77 K (which reduces the magnitude of the hot source temperature), and the use of MLI (which reduces the effective emissivity), the radiative heat loss would be reduced. In [23] it can be found that a radiative heat transfer of 50 mW/m2 is obtained when using a 10-layer MLI while the radiating surface is at 77 K, and the cold source temperature is at 4.2K.

The radiative heat transfer from the ambient (300 K) to the heat shield (77 K) is typically estimated to be around 2500 mW/m2 [23].

(4) ELECTRIC LOSSES: RESISTIVE JOINTS

Losses at the junctions of a magnet are described by the Joule effect:

$$Q_{in} = N \cdot I^2 \cdot R$$

Where N is the number of junctions, I is the rated current and R is the junction resistance.

The resistive value is a critical factor in defining joint losses. A study of the resistive values achieved in three commercial HTS tapes can be found in [22]. The three tapes tested are SuNAM, Superpower and SuperOx, and the schematic of the tested solder is depicted in Figure 23.

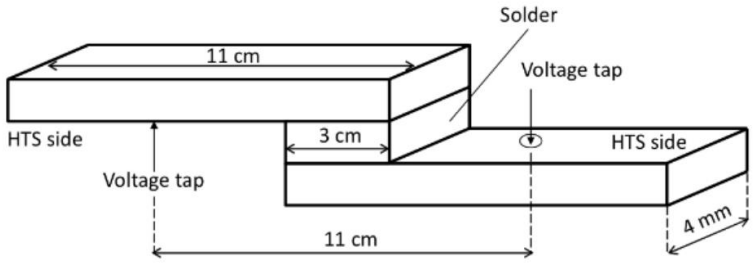

Figure 23 View of the face-to-face welded joint of two pieces of 2G HTS cable

The soldering was done face to face with a soldered area of 1.2 cm2. For the soldering process standard ethanol rosin flux and Pb39Sn61 eutectic solder were used. Additionally certain pressure was applied during the soldering process. With the method presented in this work they achieved low resistance values, of a few nΩcm2, in the case of the SuperOx tape, a resistance as low as 10 nΩcm2 was reached.

The results are shown in Figure 24. With this method a resistance of 12 nΩ is achievable if we use the same area for the soldering and the soldering is done at low pressure to avoid the degradation of the tape (assuming a value of 15 nΩcm2).

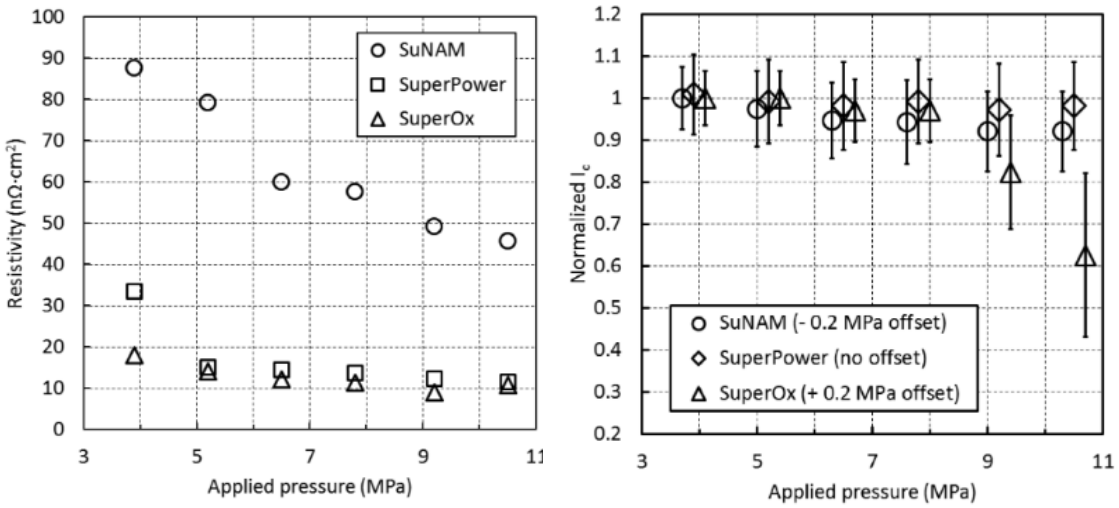

Figure 24. Dependence of joint resistivity on applied pressure (left), and Dependence of joint critical current normalized to critical current of the initial wire on applied pressure (right) [22]

Additionally, we carry out a certain number of experiments to test the value of a soldered resistance at liquid nitrogen values. The resistance value is not significant, but the difference to the copper resistance and the difference to the resistance given by the manufacturer could indicate or aid to establish a coefficient of security for the 4.2K joints.

In this case the soldering was done with In52Sn48, and a resistance of 125 nΩcm2 was achieved. Two times the indicated value from the manufacturer and an order of magnitude higher than the copper resistance. The difference with copper resistance agrees with the values obtained in [22].

That implies that the 12 nΩ resistance achieved with the method presented in [22] is reasonable with a typical soldering process.

(5) ELECTRIC LOSSES: CURRENT LEADS

Vapor-cooled current leads

A schematic of a vapor-cooled current lead is presented in Figure 25Figure 25. Vapor cooled current leads. The heat flowing into the current lead is comprised of a conduction term, and the joule dissipation generated within the current lead. A heat input of $1\frac{mW}{A}$ is the typical rule-of-thumb value for optimized vapor-cooled leads. For copper current leads, the relation of the current I_0, length l and area A is:

$$\left(\frac{I_0 l}{A}\right) \approx 2.3x10^7 \frac{A}{m}$$

And for a brass lead:

$$\left(\frac{I_0 l}{A}\right) \approx 1.2x10^7 \frac{A}{m}$$

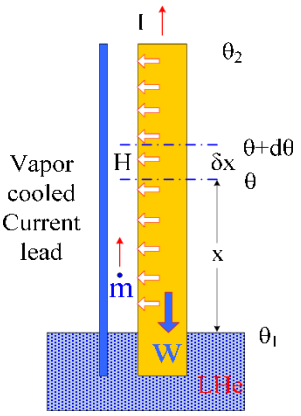

Figure 25. Vapor cooled current

HTS current leads

A schematic of an HTS current lead is presented in Figure 26, where the part of the current lead which is at a temperature between 4-70 K is substituted by an HTS extension. The refrigeration of the lead can be from helium evaporated in the magnet or by conduction, often called "dry" leads.

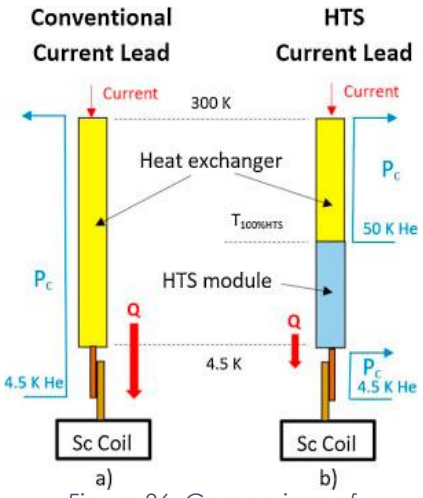

Figure 26. Comparison of copper vs HTS current leads

Vapor-cooled HTS current leads

For the vapor cooled with superconducting extensions the heat input would be:

$$Q_{Io} = \frac{\tilde{k} * A * h_L}{\widetilde{c_p} * l} \ln\left[\frac{\widetilde{c_p}(T_l - T_0)}{h_L} + 1\right]$$

The HTS must be protected in case of quench with a normal metal (typically copper) lead in parallel. Therefore, the $\tilde{k} * A$ term is modified into:

$$\left[\tilde{k} * A\right]_{lead} = \widetilde{k_{HTS}} * A_{HTS} + \widetilde{k_{copper}} * A_{copper}$$

Table 10. Parameters of HTS tape

Parameters	Values
Overall width	4 [mm]
Overall thickness	0.1 [mm]
Cross section	0.4 [mm²]
Ic (Tl) (@77-80 k @b=0.2 t)	~170 [A]
Ic (To) (@4.2 k @b=0.2 t)	~3000 [A]
$\widetilde{k_{hts}}$ **(4.2 -77 K)**	400 [W/mK]

(6) ELECTRIC LOSSES: AC LOSSES

AC losses in a superconducting material are generated due to a magnetic field and/or the transport of a current, with one or both varying over time. Three types of AC losses affecting the energy density are recognized: hysteresis, coupling and Eddy currents. AC losses generally depend on the cross-sectional shape of the conductor and the direction of the magnetic field with respect to the conductor axis.

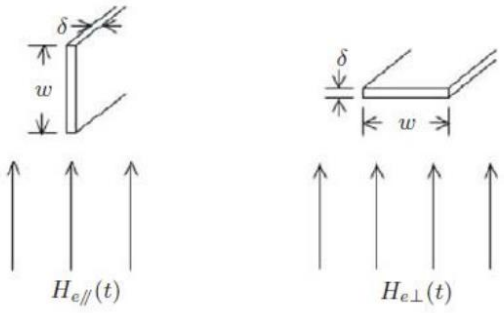

Figure 27 Field to tape orientations

Coupling losses

Coupling losses are a form of energy dissipation through the Joule effect within a multifilamentary composite. It is the result of the inter-filament current induced in that composite exposed to a time-varying magnetic field. Because the junction current flows through the resistive metal matrix and decays with time so, for simplicity, it is generally characterized through an exponential form with a single junction time constant.

Hysteresis losses

Losses due to the well-known phenomenon of hysteresis are produced by the magnetization and demagnetization of the core when the current flows in the forward or reverse direction. When the magnetizing force (current) increases, the magnetic flux increases as well. But when the magnetizing force (current) decreases, the magnetic flux does not decrease at the same rate, but less gradually.
Therefore, when the magnetizing force has reached zero, the flux density still has a positive value. To get this flux density to cancel out, the applied magnetizing force must have an opposite direction.

Computation of AC losses: Integral formulation

There are simplified formulas for the computation of AC losses in simple geometries [23]. However, if the geometry is more intricate or if more accurate superconductor properties, including the critical current's dependence on temperature and magnetic field, must be taken into account, numerical approaches are required.

A novel approach employing an integral formulation of Maxwell's equation was created by E. H. Brandt in 1994. In essence, Brandt's approach makes use of Maxwell's equations to identify an integral equation for the current density's time derivative. The integral is changed into a matrix multiplication using spatial discretization. The current density is determined by numerically integrating the resulting system of ordinary differential equations (ODEs) in time. The absence of boundary conditions, in contrast to a differential formulation, is a benefit of this method. Therefore, the equation can only be solved inside the superconductor volume. As a result, there are a lot less unknowns. Second, MATLAB or other free alternatives make it easier to solve the ODE system.

Simon Otten et al. [24] provide an open-source version of this formulation which has been adapted to fulfill the design requirements. The developed algorithm works as follows:

1. EM problem is solved in ANSYS Maxwell: The code receives from an external program the necessary inputs: geometry of the magnet, and the operating conditions (current, magnetic field distribution)
2. Data is read in MATLAB and processed: the coil is discretized in N number of tapes (equal to the number of turns), each operating at the computed current and magnetic field.
3. AC losses are computed for each tape with [24]computation method using the rectangular bar approximation. The total AC losses for the magnet are computed as the sum of the contribution of the individual tapes.

The proposed method has its own limitations mainly due to the approximation of equal magnetic field along each individual tape, which is not necessarily true in every case. To develop a more precise AC losses method there is a need to utilize 3D FEM solvers and more complex formulations, with additional computations efforts.

Computation of AC losses: Isothermal Discharge at 20K

Applying the algorithm, we compute the losses for a 10 second discharge for the base case presented in the electromagnetic design chapter, maintaining a constant temperature of 20K during the process.

Figure 28 show the results obtained, in the left part of the image the figure shows the heat input distribution along the magnet. Notice the hot spots at the top and bottom coil, which are concentrated are the outer parts of the coil. The reason is due to the direction of the magnetic field, which is more perpendicular to the tape in this area. The positive part of this is that the inner side, which has a higher working point than the outer side (lower temperature margin) has lower heat input. At the right hand side of the figure the total heat input values are shown. A symmetric solution was not achieved due to numerical limitations.

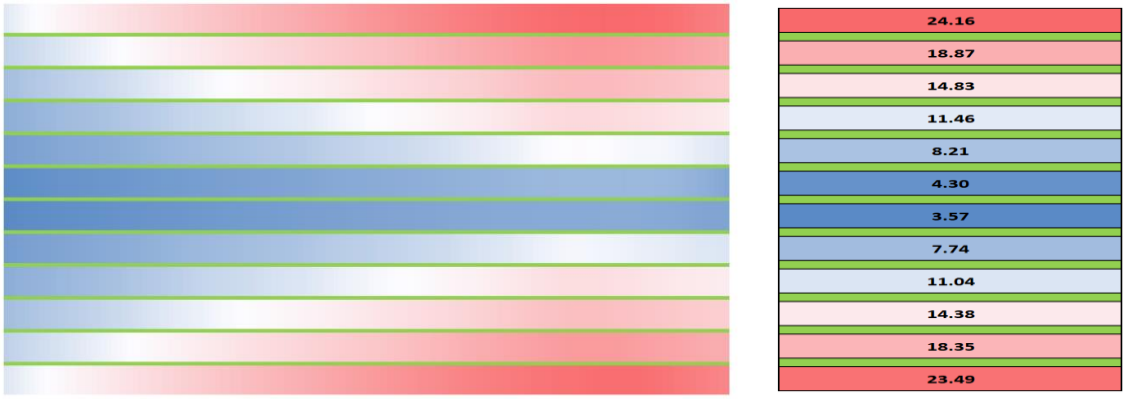

Figure 28 Heat distribution in Watss for the whole magnet during an isothermal discharge at 20K coil (left) and total amount of heat generated per coil during discharge (in W)

(7) SUMMARY OF THERMAL AND ELECTRIC LOSSES

In the previous sections the main sources of thermal losses and their computation method have been addressed. Next, we will provide a range of expected values of this losses in order to give an initial estimation of the refrigeration system size in the next section.

Table 11 Main parameters for the computation of thermal losses

	Value @ 4.2 K	Value @ 20 K	Value @ 77 K
Geometry			
Weight		40 kg.	
External Area		0.12 m^2	
Est. Number of joints		4 per double pancake (~50)	
Operating point			
Current	515A	275 A	41 A
Power (Discharge time)	10 s	10 s	10 s

Three temperatures have been considered: 4.2K(LHe), 20K(LH2) and LN2(77K). For the first two we introduce a thermal shield at 77K in the thermal losses computations. So, in addition to the heat losses presented in Table 12, there is need to evacuate the input heat at the radiation shield. This heat input will be in the range of the heat input presented for the 77K case.

Table 12. Summary of thermal losses at 4.2K, 20K and 77K

Source	Value @ 4.2 K (thermal screen @ 77K)	Value @ 20 K (thermal screen @ 77K)	Value @ 77 K
Thermal losses			
Convection	0 W	0 W	0 W
Conduction	0.2-0.3 W	0.15-0.25 W	0.5-0.7 W
Radiation	0.005-0.01 W	0.02-0.03 W	2-3 W
Electrical losses			
Splices	0.3-0.5 W	0.06-0.07 W	0.0015 W
Current leads	0.4-0.5 W	0.3-0.4 W	13-15 W
AC losses	625-650 W	150-170W	3-4 W
Total	625-655 W	150-175 W	20-25 W

From this analysis, we realize the following:

- AC losses are the main contributors of thermal losses for an HTS magnet with high power requirements.
- Although extreme AC losses are transient, and the heat is only generated during ramps. The introduction of high thermal inertia could be energy savvy, and increase the efficiency of the system. Another possibility would be to operate with high temperature margin in the tens of Kelvin.
- Heat distribution is broad and concentrated in certain points of the coils. There is need to extract that heat from where it is generated, in other words we need to reject heat locally and should minimize interference with the electromagnetic design.

2.2.3. CRYOGENIC REFRIGERATION SYSTEMS

Having defined the temperature and the dissipated power one can assess the selection of the refrigeration method of the SMES.

Refrigeration systems can be divided into two groups: open and closed systems. An open system allows energy, and matter exit and enter the system, while a closed system is isolated from the environment. Open systems are still commonly used, especially in cryogenics, where the object to be cooled is submerged in a bath of liquid cryogen [25]. However, there is an interest in substituting them for closed systems, due to efficiency and cost issues.

For this application we can foresee up to four different possibilities for the cryogen supply to the superconducting device:

- Bath-type refrigeration: In this design, a certain amount of liquid cryogen is directly injected into the system. Enthalpy change in the cryogen is used to refrigerate the material, which is kept at the vaporization temperature of the cryogen. Evaporated Helium can be used for refrigeration of parts at intermediate temperatures. The best and most important example is the current lead refrigeration. They provide a path for the current to flow from ambient temperature (power supply) to the coil (liquid Helium temperature), so it is an important input heat source. It can be reduced by following several strategies to refrigerate the current leads with the Helium vapor before letting it go out. This is the simplest way to cool down the material, but it is not typically

efficient for a long-lasting and continuous operation machine. It requires a periodic refill of cryogen, which can be expensive.

- Conductive refrigeration: One or more cryocoolers are in contact with the material to be cooled down. A cryocooler becomes cold by means of a thermodynamic cycle inside, while the refrigeration cryogen stays inside the cryocooler. Thermal contact is critical in this strategy and limited power is available for each cryocooler. Moreover, both magnetic and cryogenic systems are completely related to each other: some space close to the coils needs to be available for the cryocooler cold head. Also, as cryocoolers efficiency is reduced by magnetic fields, some shielding could be needed. Finally, accessibility for maintenance operation of cryocoolers should be taken into account during design. Because of these reasons, magnetic circuit design is linked to the thermal one in this scheme. Conductive refrigeration is also the only configuration which cannot be easily scaled in terms of cooling power. Once the design is fixed for a given cryocooler, it cannot be updated by changing it or adding higher amount of cryogen like in the other options. This should not be a drawback for a well-known product, but this work is focused on a prototype machine which could be used as the baseline for a number of updates or improvements in the future.

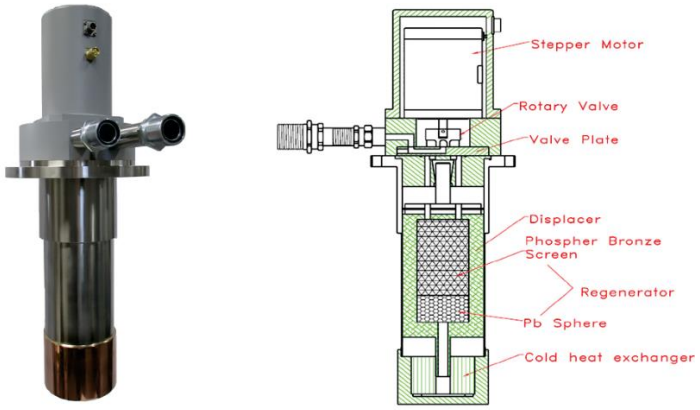

Figure 29. Image and schematic of a GM cryocooler

- Hybrid solution: One or more cryocoolers are used in this scheme, but they are not in direct contact with superconducting material, which is actually refrigerated by certain amount of liquid Helium like in the bath-type configuration. The difference is that the evaporated Helium is liquefied again by the cryocooler inside the cyclotron cryostat. Liquefied Helium returns to the bath, so in this case the objective is to keep a constant liquid level without any refill.

- Flow refrigeration: Certain amount of cryogen is cooled down and then it is pumped into the system to be cooled down. It could be an open or closed cycle; it depends if the exhaust cryogen is recovered or not. Cryogenic and superconducting systems can be designed independently. Large systems are usually based on this configuration as it allows developing a scalable cryogen liquefaction facility based on the thermodynamic cycle preferred for that specific application.

Table 13. Advantages and disadvantages of different cooling methods

	Bath-Type	Conductive	Hybrid	CSS
Advantages	Simple Highly reliable Isothermal refrigeration	Simple Low operational cost	Reliable Low operational cost Isothermal refrigeration	Autonomous system Magnetic and cooling systems are independent. Scalable power Easy maintenance High operational safety Low operational cost Isothermal refrigeration
Disadvantages	Expensive (scarce element), periodic refillments High operational cost	Magnetic and cooling system design linked Difficult maintenance Component activation Fixed thermal power	Magnetic and cooling system design linked Difficult maintenance Component activation Fixed thermal power	Complex system Higher initial cost

The commonly used configurations for the refrigeration of a magnet (liquid helium bath, conduction cooling from a cryocooler, and the hybrid/thermosyphon) were discarded due to the following reasons:

1) Cheap and autonomous operation: the unit was required to have a continuous and autonomous operation with low operational cost; therefore, the helium bath option was discarded.
2) Isothermal refrigeration: The heat produced by AC losses during the discharge of the SMES is localized and need to be rejected with accuracy, therefore for this purpose conduction refrigeration seems deficient as is not capable to extract heat locally with sufficient velocity.
3) Cryogen availability: the thermosyphon alternative is plausible and might be an alternative, however in this configuration the SMES is required to work at a constant temperature, the liquefaction temperature of the cryogen at ambient pressure. There are a few cryogen alternatives: LHe (4.2K), LH2 (20K), LNe (27K) and LN2 (77K). Helium and Neon are discarded due to their scarcity and high costs. Hydrogen is a medium-term possibility, but for this project is not considered due to safety issues. Nitrogen is the long-term ideal solution, however the energy achieved at those temperatures is modest and far from the objectives.

2.2.4. CRYOGENIC SUPPLY SYSTEM (CSS)

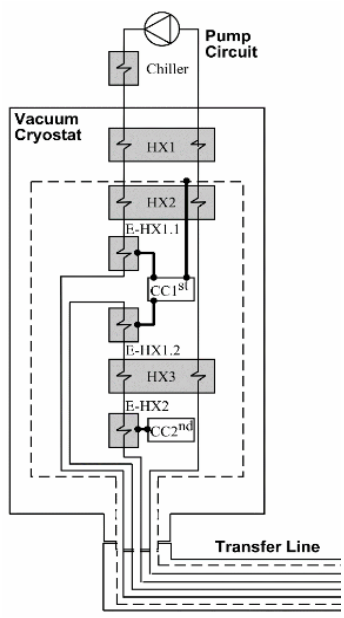

Figure 30. Cryogenic supply system [26]

Flow refrigeration was then the preferred option for this work. It provides an autonomous, cheap, compact system capable of rejecting heat locally and with the possibility of operating at different temperatures, from 4.2K to 77K. Following this concept partners of the project, CIEMAT, CERN, and CYCLOMED, has developed a cooling system based on the flow refrigeration concept called Cryogenic Supply System (CSS), which has been successfully tested in other applications.

The CSS is a closed system where a cryogen is pumped at ambient temperature (GHe in this case), goes through a series of heat exchangers recovering the heat from the returning fluid and is coupled with a cryocooler which cools the cryogen down. It has two refrigeration stages: one for the thermal shield, and another for the magnet.

The core of the CSS is a cryocooler. In the first prototype a SRDK-415D *Sumitomo* cryocooler was used. This cryocooler is based on a Gifford-McMahon cycle able to provide up to 1.5 W of cooling power at its second stage (at 4.2 K) and 35 W at its first stage (at 50 K). However, the cooling requirements for that application are different than for the present one. In the next section we will preliminarily evaluate the potential cryocooler options.

(1) CRYOCOOLER SELECTION

The cryocooler selection will depend on the cooling requirements and the operating temperature. In Table 12 we summarize these constraints for each operating point, from which we can derive the potential best alternatives:

- If the operating temperature is 20K or lower there is need to use an active thermal screen, therefore the selected cryocoolers must have two stages. For this application we preselected two cryocoolers: for operation at 10K or lower the Sumitomo RDE-418D, and for higher temperatures, but below 40-50K the Sumitomo CH-210L. Figure 31 show the heat rejection capacity map for each alternative.
- For 77K operation we selected the CH-160D2 cryocooler. Figure 32 shows the cooling capacity map.

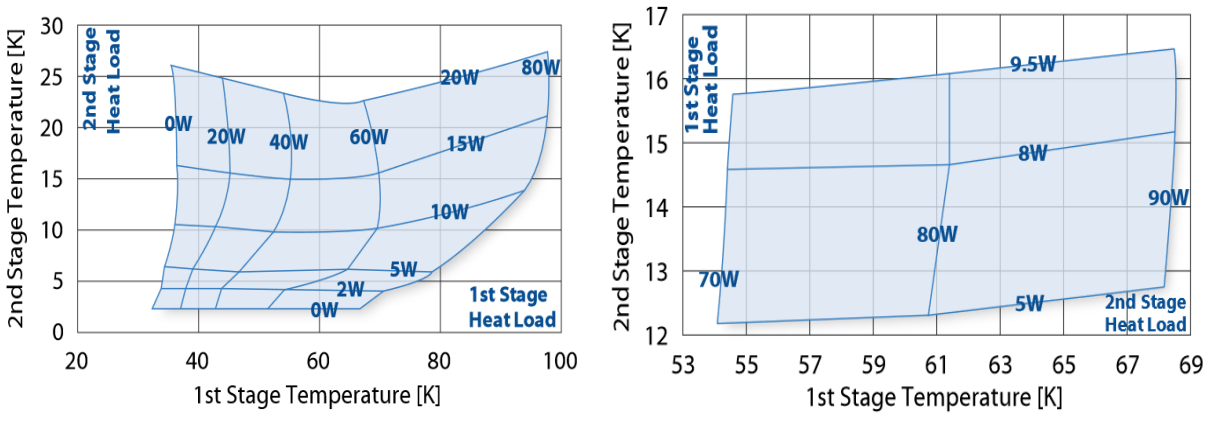

Figure 31 Heat rejections capacities as function of 1st and 2nd stage temp. for: SDRE-418D (left) & CH-210L (right)

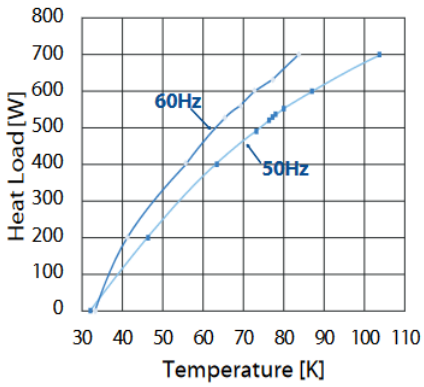

Figure 32 Heat rejections capacities as function temperature for the CH-160D2

2.3. SMES POWER CONDITIONING SYSTEM (PCS)

The SMES Power Conditioning System is in charge of exchanging energy with the grid. Along the development of SMES, different configurations of PCS have been proposed, each having their own pros and cons. They all have a grid side converter (in some cases it is the only existing device) and the power that can be exchanged with the grid is given as:

Active Power $P = V \cdot I \cdot \cos \alpha$ (4)

Reactive Power $P = V \cdot I \cdot \sin \alpha$ (5)

Where V is the grid voltage, I the phase current and α the firing angle

The first option is the thyristor-based PCS which is the simplest topology involving the smallest amount of power switches. Additionally, it uses the type of switches (thyristors), able to transport the highest currents of all electronic switches being particularly suitable for SMES, since the involved currents are very high. Control system is also very simple.

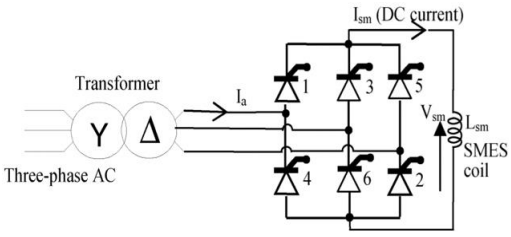

Figure 33. Thyristor-based PCS

On the drawback side, the first one is the restriction of working in the range for α of $0 < \alpha < 180$ leading to the inability of working with negative values for reactive power (injecting reactive power to the grid).

Another drawback is that the Total Harmonic Distortion (THD) is much higher than for other PCSs and also that ripple in the superconducting coil is higher, leading to bigger a.c. losses.

The second option is the Current Source Converter PCS which basically consists in a current commutator of the line current into the coil. There are usually two configurations (6 and 12 pulses) and to reduce voltage ripple, inductances and capacitors must be placed in the grid side. They are tuned to eliminate certain harmonics.

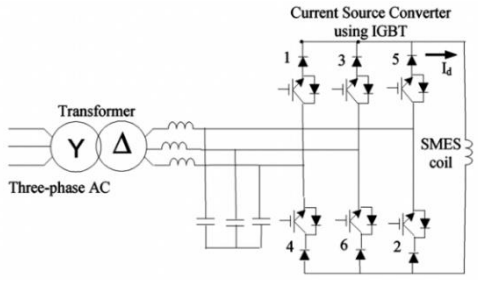

Figure 34. Current Source Converter PCS

Since the firing angle α is able to be located in the full range ($0 < \alpha < 360$) all the different combinations of active and reactive power can be achieved, even the delivery of capacity reactive power to the grid (negative reactive power).

As the system only uses a single converter, its control strategy is also simple while ripple in the superconducting coil can be relatively small, especially for the 12-pulse configuration.

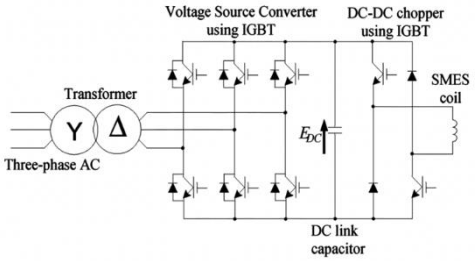

Figure 35. Voltage Source Converter PCS

Finally, the third option is the Voltage Source Converter PCS which is formed by a Gride Side Inverter based on IGBTs and a dc-dc chopper. In this case the control strategy is based on keeping a constant voltage across the dc-link capacitor and since the system includes two converters, the control strategy is more complex than for the other configurations. As for the previous type of PCS, this option allows interchanging of power in the four quadrants as α can be selected from cero to 360°. This solution is characterized by an intermediate value of THD and also a medium ripple in the voltage applied to the coil leading to moderate a.c. losses.

From the previous descriptions and also considering that at this level the core activity of the project should be concentrated in the development of the superconducting coil and its associated cryo-system, we have chosen a simplified version of the VSC in which we use a commercial bipolar power supply connected to the grid and a chopper with flywheel diodes and a load to recover the stored energy in the coil.

2.4. SUMMARY: TECHNOLOGY SELECTIONS

The technological alternatives, and selections made for the POSEIDON SMES have been stated in previous sections, which will be the based for the engineering design that will follow. Table 14 and Table 15 provides a summary of the selected technologies.

Table 14. Technological selections of POSEIDON SMES

	Selection	Description
SC Material	**2G HTS Tape**	HTS technology selected due to its **High critical temperature:** Less power required by the refrigeration system. Easier to remove AC losses. Shanghai superconductors as tape provider: best EM and good mechanical properties. Best economics. Partners have worked with them in the past which reduces risks.
Topology	**Solenoidal**	Solenoidal arrangement made of 12 double-pancake coils. This option is **easy to assemble** and easy to fabricate. **Scalability due to its** modularity.
Refrigeration	**Cryogenic Supply System (CSS)**	Flow refrigeration with CSS. Selected for its affordability, and capacity to extract **heat very close from where it is produced** (the tape) since the gas is circulated through the magnet and not removed from conduction.
PCS	**VSC & DC-DC chopper**	Selected a simplified version of the VSC with a commercial bipolar power supply connected to the grid and a chopper. Allows **Independent control of the Active and Reactive Power**. The overall THD can be quite small.

Table 15: Properties of POSEIDON SMES

SC Tape	**Company**	Shanghai SC 2G REBCO
	Critical current density @4.2K 10 T	406 A/mm²
	Critical current density @77.5K 0 T	192 A/mm²
	Bending radius	6-7 mm
	Rated Stress	300-700 MPa
	Width	4 mm
	Average Thickness	0.255 mm
Topology	**N° of pancakes**	12
	Pancake length	200 m
	Outer radius	135 mm
	Inner radius	86 mm
	Height	131 mm
EM Properties	**Operating Temperature**	20K (4.2K)
	Current density	168.2 (317) A/mm²
	Energy	77.7 (275) kJ
	Max. Magnetic field	6.08 (11.44) T
	Max. stress	194 MPa
Thermal Losses	**Thermal Losses @20K (4.2K)**	0.2-0.4 W
	Electrical Losses @20K (4.2K)	150-170 W
	Refrigeration type	Flow refrigeration

3. CONCLUSIONS

The electrification of the economy is a reality that will impact (and is impacting) the condition of the transportation sector, including maritime transport. Ship grids are evolving in complexity, developing new issues such as complex control of the power quality, and power flow. Some of these arising problems can be addressed with the addition of Energy Storage Systems (ESS) in the ship microgrid. We realize the following:

1. The integration of high energy density ESS, such as Li-ion batteries, in ships is rapidly improving, however there are specific situations that cannot be addressed by this type of ESS, and there is need for high specific power systems. It is the case, for example, of a short river ferry which has a power profile with a high number of duty cycles.
2. Being a novel industry in the maritime sector, there is little regulation on ESS, and most of it is focused on electrochemical batteries. Therefore, the ESS designer must work with regulators, and/or provide their insights, in order to address the marinization of these novel technologies. We have identified the most relevant existing directives that will establish the guidelines and minimum conditions for correct and safe integration of the SMES on-board.
3. According to state-of-the-art information and use case we have established a range of energy and power values which are attractive for an SMES with on-board application. For the SMES developed in POSEIDON we are targeting the low range of energy, limiting this first development to 150-250 kJ.

From the design point of view, a SMES consists of four basic subsystems: The Magnet, the Cooling Device, the Power Condition Converter and the Control & Protection System. Regarding the magnet we derive the following conclusions:

4. It has been decided to use a High Temperature Superconducting (HTS) Magnet since it represents a number of promising advances over using a Low Temperature Superconducting Magnet. The choice of an HTS magnet has deep implications on the rest of SMES subsystems.
5. Within the group of HTS there are different potential providers, but 3 were preselected due to previous collaborations and already acquired knowhow by the partners in the HTS tape handling of those companies. Among the preselected providers, the partners decided for Shanghai Superconductors since their HTS tape exhibits the best electromagnetic, and mechanical properties and a relative economic price.
6. There are a number of alternatives for the magnet construction, Nevertheless, the limitation of the maximum length in which the superconducting tapes are delivered, practically imposed a magnet fabrication based on double pancakes which are series connected to configure a certain topology.
7. There are also two possible configurations for the magnet topology: the Solenoid and the Toroid. The first can have a very reduced stray field and also the field in the superconductor is in the favorable direction where the critical current is higher. On the contrary, the required footprint is bigger, and the assembly complexity is also much higher than for the second alternative which lacks of previous advantages but has net balanced forces and a higher simplicity.
8. For both topologies the presence of a core can significantly increase the stored energy and reduce stray fields. In fact, for the POSEIDON SMES it has been proposed to use a magnet core with an intermediate permeability between iron and air in a proportion which must be optimized for the application.
9. The final topology is a solenoid magnet based on several modular doble pancakes. Each pancake is made by 2 tapes of 100 m length, the final geometry parameters of

the pancakes is 135 mm of outer radius, 86 mm of inner radius and 144 turns. Several magnet configuration and operation temperatures are studied to obtain the maximum stored energy of 275.8 kJ at 4.2K with 12 double pancakes.

10. Mechanical stress distribution in the magnet is evaluated analytically and with FEM models. A stress less than 200 MPa is obtained with both methods, with a high security margin compared to the limit stress of the HTS material selected, 400 MPa
11. There are several details concerning the manufacturing process of a coil made of HTS tape that must be checked in advance. Special care should be taken about the handling methodology, winding procedure and joining parameters. All these points are highly sensitive to the actual HTS tape and its performance. Limited experience and information is available even from the supplier, so previous tests should be made for this specific application.

The cryogenic system sets the selected operating temperature of the HTS magnet, for that it must be capable of rejecting the heat produced in the SMES. We distinguish two types of heat losses: thermal and electric, each again subdivided in different groups depending on their physical origin. From the cryogenic analysis:

12. We provided an estimate of these losses at 3 temperatures: 4.2K, 20K, and 77K. We derive from this analysis that the main source of heating would be during current transients due to AC losses.
13. AC losses are the most predominant heat losses of the SMES, therefore a detailed model was developed for their precise computation. This model has been validated against state-of-the-art sources, but only for short samples. The test benches developed for validating the manufacturing process will be used to measure electrically and thermally the AC losses of larger samples.
14. Selecting the operating temperature and estimating the heat losses, there are a different number of cooling methods than could be developed to maintain the desired conditions. Among those potential systems we have considered that the Cryogenic Supply System is the best alternative since it provides: cheap and autonomous cooling, isothermal cooling in the coils, and provides a broad operating temperature range.

Three different alternatives for the Power Conditioning Subsystem have been analyzed:

15. A thyristor based (discarded because of the high dc ripple and inability to work in four quadrants) A Current Source (discarded for its higher complexity for this concrete application) and a Voltage Source which is the one selected in a simplified version in which the ac-dc converter is replaced with a programmable existing power supply.

4. REFERENCES

[1] J. H. Williams *et al.*, "Carbon-Neutral Pathways for the United States," *AGU Adv.*, vol. 2, no. 1, p. e2020AV000284, Jan. 2021, doi: 10.1029/2020AV000284.

[2] IEA, "IEA (2022), Transport," Paris, 2022. [Online]. Available: https://www.iea.org/reports/transport.

[3] International Maritime Organization, "International Maritime Organization: Prevention of Air Pollution from Ships." [Online]. Available: https://www.imo.org/en/OurWork/Environment/Pages/Air-Pollution.aspx.

[4] S. G. Jayasinghe, L. Meegahapola, N. Fernando, Z. Jin, and J. M. Guerrero, "Review of Ship Microgrids: System Architectures, Storage Technologies and Power Quality Aspects," *Invent. 2017, Vol. 2, Page 4*, vol. 2, no. 1, p. 4, Feb. 2017, doi: 10.3390/INVENTIONS2010004.

[5] M. U. Mutarraf, Y. Terriche, K. A. K. Niazi, J. C. Vasquez, and J. M. Guerrero, "Energy Storage Systems for Shipboard Microgrids—A Review," *Energies 2018, Vol. 11, Page 3492*, vol. 11, no. 12, p. 3492, Dec. 2018, doi: 10.3390/EN11123492.

[6] S. Jafarzadeh and I. Schjølberg, "Emission Reduction in Shipping Using Hydrogen and Fuel Cells," *Proc. Int. Conf. Offshore Mech. Arct. Eng. - OMAE*, vol. 10, Sep. 2017, doi: 10.1115/OMAE2017-61401.

[7] "Energy Storage Technologies for Electric Applications." http://www.sc.ehu.es/sbweb/energias-renovables/temas/almacenamiento/almacenamiento.html (accessed Jun. 12, 2023).

[8] EMSA European Maritime Safety Agency, "STUDY ON ELECTRICAL ENERGY STORAGE FOR SHIPS," 2019.

[9] N. Bennabi, H. Menana, J. F. Charpentier, J. Y. Billard, and B. Nottelet, "Design and Comparative Study of Hybrid Propulsions for a River Ferry Operating on Short Cycles with High Power Demands," *J. Mar. Sci. Eng. 2021, Vol. 9, Page 631*, vol. 9, no. 6, p. 631, Jun. 2021, doi: 10.3390/JMSE9060631.

[10] K. Kim, J. An, K. Park, G. Roh, and K. Chun, "Analysis of a Supercapacitor/Battery Hybrid Power System for a Bulk Carrier," *Appl. Sci. 2019, Vol. 9, Page 1547*, vol. 9, no. 8, p. 1547, Apr. 2019, doi: 10.3390/APP9081547.

[11] American Bureau of Shipping, "USE OF SUPERCAPACITORS IN THE MARINE AND OFFSHORE INDUSTRIES," 2017.

[12] N. Mjøs *et al.*, "DNV GL Guideline for large maritime battery systems," 2014. Accessed: Jun. 12, 2023. [Online]. Available: www.dnvgl.com.

[13] Narve Mjøs, Sverre Eriksen, Andreas Kristoffersen, Gerd Petra Haugom, and Asmund Huser, "DNV GL Handbook for Maritime and Offshore Battery Systems," 2016. Accessed: Jun. 12, 2023. [Online]. Available: www.dnvgl.com.

[14] U. C. of E. on the T. of D. Goods and U. E. Secretariat, "Recommendations on the transport of dangerous goods.: Model Regulations.: Volume 1," *Recomm. Transp. Danger. goods - Model Regul.*, vol. Volume I, pp. 49–181, 2019, Accessed: Jun. 12, 2023. [Online]. Available: https://digitallibrary.un.org/record/3830095.

[15] "IEC 62619:2022 | IEC Webstore." https://webstore.iec.ch/publication/64073 (accessed Jun. 12, 2023).

[16] "Deliverables - Current Direct." https://www.currentdirect.eu/deliverables/ (accessed Jun. 12, 2023).

[17] Official Journal of the European Union, *DIRECTIVE 2013/35/EU OF THE EUROPEAN*

PARLIAMENT AND OF THE COUNCIL. 2013.

[18] DR Conover *et al.*, "Protocol for Uniformly Measuring and Expressing the Performance of Energy Storage Systems," 2016.

[19] L. Rossi and C. Senatore, "HTS accelerator magnet and conductor development in europe," *Instruments*, vol. 5, no. 1, 2021, doi: 10.3390/INSTRUMENTS5010008.

[20] J. CICERON, "High energy density Superconducting Magnetic Energy Storage with second generation high temperature superconductors," University of Grenoble, 2019.

[21] R. Radebaugh, "Cryocoolers: the state of the art and recent developments," *J. Phys. Condens. Matter*, vol. 21, no. 16, p. 164219, 2009, [Online]. Available: https://doi.org/10.1088%2F0953-8984%2F21%2F16%2F164219.

[22] N. N. Balashov *et al.*, "Low-Resistance Soldered Joints of Commercial 2G HTS Wire Prepared at Various Values of Applied Pressure," *IEEE Trans. Appl. Supercond.*, vol. 28, no. 4, Jun. 2018, doi: 10.1109/TASC.2018.2806388.

[23] Y. Iwasa, "CHAPTER 7 AC AND OTHER LOSSES," in *Case studies in superconducting magnets: design and operational issues; Second edition*, Springer, 2009, pp. 399–466.

[24] S. Otten and F. Grilli, "Simple and Fast Method for Computing Induced Currents in Superconductors Using Freely Available Solvers for Ordinary Differential Equations," *IEEE Trans. Appl. Supercond.*, vol. 29, no. 8, Dec. 2019, doi: 10.1109/TASC.2019.2949240.

[25] M. Atrey, *Cryocoolers Theory and Applications: Theory and Applications*. 2020.

[26] F. Haug, "The AMIT magnet cryosystem," in *Panel review meeting*, 2012, pp. 10–12.